AN ABSTRACT OF THE THESIS OF

Soon-Ung Park for the degree of Doctor of Philosophy

in Atmospheric Sciences presented on March 29, 1978

Title: Influence of Stratification and Accelerations on Boundary Layer Production of Vertical Motion

Abstract approved Redacted for Privacy
Larry J. Mahrt

The influence of boundary layer pumping on an externally-forced synoptic-scale flow is examined. The results follow earlier theories of stratified incompressible Boussinesq flow. These theories state that the spin-down time scale and the penetration depth of the influence of boundary layer pumping are inversely proportional to the stratification and directly proportional to the horizontal length scale of the flow. However, the present development is performed in isentropic coordinates which allow estimates applicable to the atmosphere, and implicitly includes nonlinear influences due to tilting and vertical advection. This analysis indicates that boundary layer pumping could be important synoptically in the lower troposphere under conditions of significant surface stress and tropospheric stratification.

The influence of stratification and accelerations on synoptic-scale, boundary layer production of vertical motion is examined for the case of oscillating boundary-layer flow driven by time-dependent, horizontally-periodic surface temperature perturbations. It is found that only very strong stratification can significantly reduce the boundary layer pumping through pressure adjustments within the boundary layer. As a step in understanding the complicated dynamics of the structure of

accelerated stratified boundary layers, order-of-magnitude analyses of variables for each layer are examined. This structure depends on the relative magnitude of the non-dimensional forcing frequency and the product of the stratification parameter and Ekman number. Applications to both synoptic and diurnal atmospheric circulations are considered.

Influence of Stratification and Accelerations on Boundary Production of Vertical Motion

by

Soon-Ung Park

A THESIS

submitted to

Oregon State University

in partial fulfillment of
the requirements for the
degree of

Doctor of Philosophy

Completed March 1978

Commencement June 1978

APPROVED:

Redacted for Privacy

Associate Professor of Atmospheric Sciences
in charge of major

Redacted for Privacy

Chairman of the Department of Atmospheric Sciences

Redacted for Privacy

Dean of Graduate School

Date thesis is presented March 29, 1978

Typed by Susan Queirolo for Soon-Ung Park

ACKNOWLEDGMENTS

I wish to express my sincere appreciation and gratitude to my major professor, Dr. Larry Mahrt for his constant guidance, perseverance and constructive criticisms throughout my doctoral program.

I am indebted and express appreciation to members of my doctoral committee for their cooperation and supervision, and especially to Dr. John Allen for his many helpful suggestions.

Finally, a very special thanks to my wife, Sookja for the many sacrifices, concerns and disappointments which she has shared with me throughout the course of this doctoral study.

This research was supported by Research Grant DES 73-06540 A01 and ATM 77-07623, Atmospheric Sciences Section, National Science Foundation.

TABLE OF CONTENTS

I. Introduction 1
Definition and Importance of the Problem. 1
Review of Early Studies 2
Purpose of This Study 7

II. Spin-Down Problem With Quasi-Geostrophic Approximation 8
Governing Equations in Isentropic Coordinates 9
The Solution With Horizontal Harmonic Forcing 20
Free Flow Response to Diurnally-Varying Boundary Layer Pumping. 25

III. Time Oscillating Stratified Boundary Layer 28
Governing Equations 29
Possible Types of Natural Boundary Layers 30
Boundary Layers Driven by the Surface Temperature Forcing . 33
Approximate Solutions 42

IV. Summary and Conclusions. 69
Bibliography. 72
Appendix I: Quasi-geostrophic Potential Vorticity Equations. 76
Appendix II: Governing Equations for the Stratified Boundary Layer 78
Appendix III: Parameterization of Radiation. 82
Appendix IV: Solution of Cubic Equation. 87
Appendix V: Boundary Layers Driven by Oscillating Basic Flow 89

LIST OF ILLUSTRATIONS

Figure		Page
II-1	Profiles of stability parameters for 50mb layers from 900-200mb and 25mb layers from 200-100mb. Layer stabilities are scaled with respect to values in lowest layer ((900-850mb). Profiles are averaged over the 38 U.S. radiosonde stations whose surface pressure remains above 900mb. Each station profile is the average of 10 Januarys, 1946-55 (see Gates, 1961, for analyses of additional stability parameters for a slightly different data set).	10
II-2	Spin-down of relative vorticity (scaled with respect to the height-independent initial value) at different levels in the free flow. Plots are labeled according to their potential temperature excess and elevation above the boundary layer top.	24
II-3	Spin-down of scaled relative vorticity. Plots are labeled according to number of days after initiation of spin-down.	24
II-4	As in Fig. II-2 except the diurnally-varying pumping efficiency.	27
III-1	Oscillating boundary layers in parameter space $(m,\hat{\omega})$. Subdivisions are facilitated by two-term balances in Eq. (III-4).	31
III-2	Scaled amplitude of the cross-isobar flow Eq. (III-23-d) as a function of height for several different values of m.	46
III-3	Scaled amplitude of the vertical velocity Eq. (III-23-e) as a function of height for several different values of m.	47
III-4	Sea surface temperature anomalies for summer (top) and fall (bottom) of 1961 where stippling indicates warm anomalies (>1°F) and shading cold anomalies (After Namias, 1976).	49
III-5	Subdivisions of the oscillating Lineykin layer in parameter space (m,ω).	52
III-6-a	Scaled amplitude of the cross-isobar flow Eq. (III-25-d) as a function of height for several different values of m and $\hat{\omega} = 10^{-1}$.	55

LIST OF ILLUSTRATIONS (cont'd)

III-6-b	Scaled amplitude of the vertical velocity Eq. (III-25-e) as a function of height for several different values of m and $\Omega = 10^{-1}$.	56
III-7-a	As in Fig. III-6-a except for several different values of Ω and $m = 4 \times 10^{-2}$.	57
III-7-b	As in Fig. III-6-b except for several different values of Ω and $m = 5 \times 10^{-2}$.	58
III-8-a	Scaled amplitude of the cross-isobar flow Eq. (III-29-d) as a function of height for several different values of m and $\Omega = 0.3$.	62
III-8-b	As in Fig. III-8-a except for several different values of Ω and $m = 10^{-2}$.	63
III-9-a	Scaled amplitude of the vertical velocity Eq. (III-29-e) as a function of height for several different values of m and $\Omega = 0.3$.	65
III-9-b	As in Fig. III-9-a except for several different values of Ω and $m = 10^{-2}$.	66
III-10	Scaled amplitude of the vertical velocity versus Ω evaluated at the top of the classical Ekman layer, $\eta = 4$. Each curve represents a specific value of m.	67

LIST OF SYMBOLS

Ω_o	Basic angular velocity
E	Ekman number
f	Coriolis parameter
u	x-component velocity
v	y-component velocity
w	Vertical velocity
M	Montgomery stream function
T	Absolute temperature
θ	Potential temperature
p	pressure
ρ	Air density
R	Gas constant
C_p	Specific heat of air at constant pressure
κ	$\frac{R}{C_p}$
P_{oo}	Reference pressure 1000mb
t	Time
g	Gravitational acceleration
N	Brunt-Väisälä frequency
γ	Actual lapse rate
Γ_d	Dry adiabatic lapse rate
$\overline{(\ )}$	Mean quantity
$(\ )'$	Perturbation quantity
L	Horizontal length scale
τ	Time scale
H	Scale height
$\Delta\theta$	Potential temperature thickness
θ_o	Potential temperature at the bottom
R_o	$\frac{\overline{U}}{\overline{f}L}$, Rossby number
B	Stratification parameter
L_R	Rossby radius of deformation
F	Ekman pumping efficiency
$\hat{\alpha}$	Angle between surface geostrophic wind and actual wind

LIST OF SYMBOLS (cont'd)

C_D	Surface drag coefficient
h	Boundary layer depths
$\mathfrak{k}$	Horizontal wave number
k	Wave number in x-direction
l	Wave number in y-direction
t_e	Spin-down time scale
ε	Ratio of diurnal amplitude and time-mean Ekman pumping efficiency
$\hat{\omega}$	Nondimensional forcing frequency
m	B^2E, Product of the stratification parameter and the Ekman number
η	Stretched vertical coordinate
δ	Thickness of boundary layer
K	Eddy exchange coefficiency
K_H	Thermal eddy exchange coefficiency
$\hat{\Delta\theta}$	Scaled amplitude of the potential temperature perturbation
α_S	Inverse thickness of the thermal Stokes layer
α_L	Inverse thickness of the oscillating Lineykin layer
$\alpha_{1,2}=\mu_{1,2}$	Inverse thickness of the oscillating stratified Ekman layer
$( )_S$	Thermal Stokes-layer variable
$( )_L$	Lineykin-layer variable
$( )_\varepsilon$	Ekman-layer variable
δ^*	Thickness of the oscillating stratified Ekman layer
ℓ^*	Vertical wavelength of the oscillating stratified Ekman layer
δ_ε	$\left(\frac{2K}{f}\right)^{\frac{1}{2}}$, Thickness of the classical Ekman layer
$( )_o$	Basic state variable
Pr	Prandtl number
Q_R	Radiational heating or cooling rate per unit mass
F_λ	Net upward terrestrial flux at the wavelength λ
U_λ	Upward terrestrial radiative flux at the wavelength λ
G_λ	Downward terrestrial radiative flux at the wavelength λ
B_λ	Plank function
a_λ	Volume absorption coefficient at the wavelength λ

LIST OF SYMBOLS (cont'd)

a_s	Volume absorption coefficient for the strongly absorbed group
a_w	Volume absorption coefficient for the weakly absorbed group
A_R	Radiative relaxation time constant
K_R	Radiational diffusion coefficient
σ	Stefan-Boltzmann constant
ζ_g	Geostrophic vorticity
ζ	Relative vorticity

INFLUENCE OF STRATIFICATION AND ACCELERATIONS ON BOUNDARY LAYER PRODUCTION OF VERTICAL MOTION

I. INTRODUCTION

A. Definition and Importance of the Problem

Interest in vertical motion induced by frictionally-driven convergence and divergence in the planetary boundary layer has increased considerably in recent years. The actual magnitude of these motions is small, but they play a crucial role in a wide variety of atmospheric phenomena. These include synoptic-scale precipitation patterns, the triggering of moist convection, lifting of suspended particles and passive tracers in the boundary layer, and the initiation of secondary circulations.

The planetary boundary layer is usually defined as the atmospheric layer adjacent to the ground which is directly and significantly affected by turbulent exchange with the surface. However, we will consider the planetary boundary layer as that layer which is directly or indirectly (through secondary circulations) significantly influenced by turbulent transports from the surface. In this layer, air motions are induced by the large-scale atmospheric horizontal pressure gradients, by the diurnal variation of radiative heating, and by secondary circulations.

One of the simplest solutions of the planetary boundary layer flow is the Ekman solution, which represents a balance between the pressure gradient, the Coriolis and the turbulent stress terms. This solution is valid only when the influences of the static stability and accelerations are small compared with Coriolis effects. In the real

atmosphere, however, motions are generally transient, and the atmosphere is usually stratified. Thus, consideration of accelerations and stratification is very important in the examination of atmospheric flows.

The vertical motion at the top of the Ekman boundary layer is often referred to as Ekman pumping. This Ekman pumping is thought to be proportional to the free flow geostrophic vorticity (Charney and Eliassen, 1949). The influence of Ekman pumping on the overlying free flow has been demonstrated in Ekman spin-up (or spin-down) theory (Greenspan and Howard, 1963; Holton, 1965; Sakurai, 1969; Walin, 1969; Buzyna and Veronis, 1971). Since atmospheric flow is characterized by a small turbulent Ekman number, the above spin-down process is far more effective than direct turbulent diffusion of vorticity. Thus, boundary layer pumping is thought to be an important feedback mechanism between large and turbulent scales of motions. The underlying physical basis of this theory is that with positive geostrophic relative vorticity, frictionally-induced rising motion induces vortex contraction aloft, resulting in destruction of geostrophic vorticity. This, in turn, decreases boundary layer pumping and thus leads to spin-down.

B. Review of Early Studies

It is useful to first discuss the various aspects of coupling between boundary layer pumping and the free atmosphere in more detail, in a framework applicable to the earth's atmosphere.

i) Homogeneous case

Greenspan and Howard (1963) considered a homogeneous, in-

compressible fluid, and showed that the whole column of fluid responds to the Ekman pumping. They also showed that there are three distinct stages corresponding to three different physical mechanisms. The first stage, of duration Ω_0^{-1}, is the development of Ekman boundary layers resulting from the stresses on the boundaries; the quantity Ω_0 is the basic angular velocity of the system. In the second stage, the interior fluid spins up to within e^{-1} of the new notation rate during the time scale $\Omega_0^{-1}E^{-\frac{1}{2}}$, where E is the Ekman number. The third stage is the decay of the residual inertial oscillations through viscous diffusion occurring over time scale $\Omega_0^{-1}E^{-1}$. An example of the analogy of these processes to flow in the atmosphere is as follows: Suppose that the atmosphere is initially at rest, and then flow is generated by differential heating. Due to stresses at the earth's surface, a planetary boundary layer will develop during the time scale f^{-1}, where f is the Coriolis parameter. Then secondary circulations will be set up due to frictional convergence and divergence within the planetary boundary layer. The flow across the isobars in the boundary layer will require compensating return cross-isobar flows in the free atmosphere. Due to the Coriolis force, this return cross-isobar flow opposes the main flow of the free atmosphere; accordingly, the circulation of free flow diminishes. Hence, the cross-isobar flow spins down as the flow adjusts to a new geostrophic equilibrium. In practice, the atmosphere is too transient for the third diffusive stage to be of interest. Since the turbulent diffusion of vorticity in the free atmosphere is too slow to be of interest, the spin-down time may be defined as the time required for the bulk of the cross-isobar flow to diminish to e^{-1} of its initial

value.

ii) Stratified Free Flow

The spin-down process of a stratified atmosphere, however, differs from the corresponding process for a homogeneous atmosphere. For a stratified fluid, considered by Holton (1965), Barcilon and Pedlosky (1967, a, b), Walin (1969), and Buzyna and Veronis (1971), the intensity of secondary circulations induced by the Ekman pumping decreases with height. Thus, flow above a certain height is only weakly affected by spin-down processes. Walin (1969) and Buzyna and Veronis (1971) have also shown that the penetration depth scale of circulations induced by the Ekman pumping increases with the horizontal scale of the flow.

Phillips (1963) showed that the stratification generally has an important effect on synoptic scales in the atmosphere. Only weakly stratified flows with large horizontal length scales behave to a first approximation as a homogeneous fluid. The spin-down rate of a stratified fluid is faster than that of a homogeneous fluid because the adjustment is limited to the layers near the boundaries instead of to the whole fluid column as in the case of a homogeneous fluid. The physical reason for this behavior is that in a stably stratified atmosphere, the adiabatic temperature or density changes, caused by the vertical motion induced in the boundary layer, correspond to pressure adjustments through the hydrostatic relationship. For a given magnitude of Ekman pumping, a greater basic stratification will yield stronger pressure adjustments. Therefore, the spin-down will occur faster.

The spin-down time scale of a stratified atmosphere is more complicated than the corresponding process for a homogeneous atmosphere.

At some reference time the air has cross-isobar flow ΔV. This cross-isobar flow ΔV usually decreases with height due to the stratification. After a time interval of $O(E^{-\frac{1}{2}}f^{-1})$ which corresponds to the spin-down time scale of a homogeneous atmosphere, the cross-isobar flow at each level decreases to the value of $\varepsilon\Delta V$, where ε is less than unity and decreases with height. The spin-down time is, therefore, defined as the time required for the cross-isobar flow to decrease to $e^{-1}\varepsilon\Delta V$. Thus, the spin-down time for a stratified atmosphere may differ from level to level. The stratified fluid in some regions far away from the boundary will not have been spun down before a diffusion time has elapsed. Thus, it is worthwhile to examine the penetration depth scale of boundary layer pumping in a stratified atmosphere.

iii) Stratified Boundary Layer

So far we have discussed the different behavior of spin-down processes for the stratified and homogeneous free atmosphere, but have neglected effects of stratification in the boundary layer. All of those studies mentioned above utilize the conventional parameterization of Ekman pumping for a neutrally stratified boundary layer, i.e. the boundary layer pumping is proportional to the relative geostrophic vorticity. For the stratified boundary layer, however, the boundary layer pumping is altered by pressure adjustments associated with the stratification within the boundary layer. Such adjustments are usually neglected on the basis that their magnitudes are small. However, a number of studies indicate they may be important in synoptic-scale circulations if the stratification is sufficiently large (Lineykin, 1955; Stommel and Veronis, 1957; Barcilon and Pedlosky, 1967 a, b; Leetmaa, 1971; Kuo,

1973, 1975). In this case, the convergence in the Ekman layer is almost comparable to the divergence in the Lineykin layer (the layer participating in the secondary circulations). As stratification increases, the Lineykin layer's effect is simultaneously felt within the Ekman layer; thus, significant pressure adjustments might occur within the Ekman boundary layer.

iv) Influence of Accelerations

Real wind observations suggest the importance of diurnally-induced accelerations. At some elevations above the night time boundary layer, air flow often reaches a maximum speed at night and a diurnal minimum during the day. Several models have been developed to explain this behavior, such as the diurnally-varying eddy viscosity with constant geostrophic wind (Buajitti and Blackadar, 1957; Estoque, 1963; Krishna, 1968), constant eddy viscosity with diurnally-varying geostrophic wind (Holton, 1967), diurnally-varying viscosity with specified time dependent geostrophic wind for neutral stability (Paegle and Rasch, 1973). Although each of these mechanisms is an important contributing factor, they cannot fully account for the observed wind. One important factor which is disregarded in the above models may be the effect of stable stratification in the boundary layer arising from the temperature and pressure changes produced by the frictionally-induced vertical motions.

While accelerations can significantly enhance frictionally-driven vertical motions (Young, 1973; Mahrt, 1975) the influence of stratification may significantly alter the character of such vertical motions (Kuo, 1973, 1975; Weatherly, 1975; Lykosov, 1972). Thus, we

emphasize the influence of the stable stratification on the production of boundary pumping with accelerations. For example, the so called nocturnal jet may involve stratification influences which have not been previously considered.

C. Purpose of This Study

There are two problems examined in this study. First, in Sec. II we examine the influence of boundary layer pumping with synoptic-scale forcing on the free flow, and determine the penetration depth scale of boundary layer pumping in a stratified atmosphere by using the conventional parameterization of Ekman pumping. Secondly, in Sec. III we investigate the boundary layer production of vertical motion, allowing for influences of accelerations and pressure adjustments within the boundary layer.

II. SPIN-DOWN PROBLEM WITH QUASI-GEOSTROPHIC APPROXIMATION

In this section, we construct solutions of spin-down which allow us quantitative comparison with atmospheric flows and which include non-linear tilting and vertical advection terms. Previous analytical theories have not permitted quantitative comparisons with the atmosphere and have neglected all nonlinear effects. This neglect has been justified by scale analyses of homogeneous flow. However, this scale analysis breaks down in the lower part of a stratified flow where vertical gradients are large.

We first derive the quasi-geostrophic potential vorticity equation for Boussinesq flow in isentropic coordinates. We then solve the quasi-geostrophic potential vorticity equation for synoptic-scale, horizontally-harmonic motion by imposing the conventional Ekman pumping law as the bottom boundary condition.

The spin-down problem developed in isentropic coordinates, although more general, follows the same mathematical procedures used with earlier theories developed in the z-coordinate (Holton, 1965; Walin, 1969; Buzyna and Veronis, 1971). An additional advantage of isentropic coordinates may be seen by comparing the linearized quasi-geostrophic potential vorticity equations developed in each coordinate system (see Appendix I). We note that the stability parameter must be assumed constant in either system in order to reduce the equations to a mathematically tractable form. In the lower atmosphere, the stability parameter in the isentropic vertical coordinate varies more slowly with height than in the other vertical coordinate systems. This is conven-

iently true in the lower troposphere where the spin-down problem is of significance. This is demonstrated in Fig. II-1, which is obtained from January radiosonde data averaged over ten years (U.S. Weather Bureau, 1957) and 38 U.S. stations in a manner similar to the analysis of Gates (1961).

A. Governing Equations in Isentropic Coordinates

Consider the atmospheric flow of a frictionless, adiabatic, hydrostatic fluid in an isentropic coordinate rotating with constant angular velocity f/2. The equations of motion (e.g. Thompson, 1961) are:

$$\frac{\partial u}{\partial t} + u\frac{\partial u}{\partial x} + v\frac{\partial u}{\partial y} - fv = -\frac{\partial M}{\partial x} \qquad \text{(II-1)}$$

$$\frac{\partial v}{\partial t} + u\frac{\partial v}{\partial x} + v\frac{\partial v}{\partial y} + fu = -\frac{\partial M}{\partial y} \qquad \text{(II-2)}$$

$$\frac{\partial M}{\partial \theta} = C_p T/\theta \qquad \text{(II-3)}$$

$$M = C_p T + gz \qquad \text{(II-4)}$$

$$\theta = T\left(\frac{P_{oo}}{p}\right)^{\kappa} \qquad \text{(II-5)}$$

$$\frac{\partial}{\partial t}\left(\frac{\partial P}{\partial \theta}\right) + u\frac{\partial}{\partial x}\left(\frac{\partial P}{\partial \theta}\right) + v\frac{d}{\partial y}\left(\frac{\partial P}{\partial \theta}\right) + \frac{\partial P}{\partial \theta}\left(\frac{\partial u}{\partial x} + \frac{\partial v}{\partial y}\right) = 0 \qquad \text{(II-6)}$$

where all horizontal velocities and gradients are taken on a constant θ surface. Eqs. (II-1) and (II-2) are the equations of motion along the x and y directions on an isentropic surface, Eq. (II-3) is the hydrostatic equation, Eq. (II-4) is the definition of the Montgomery stream function, Eq. (II-5) is Poisson's equation and Eq. (II-6) is the mass

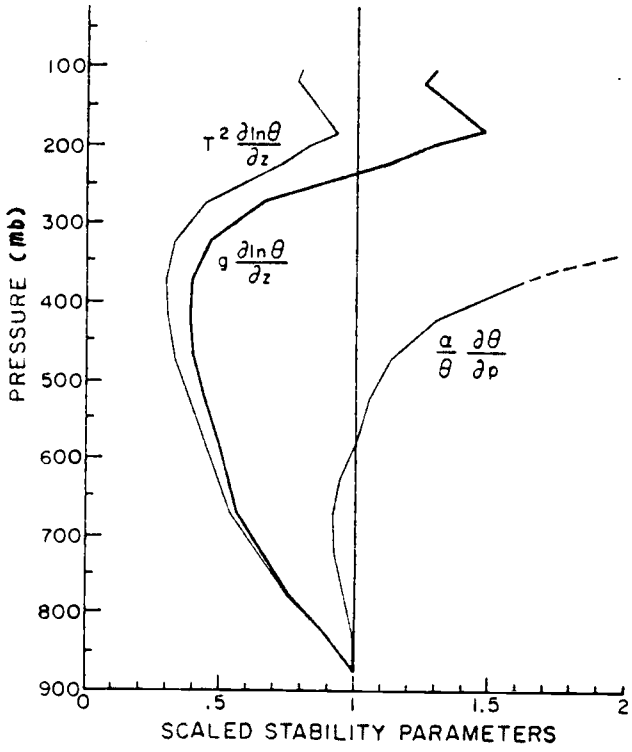

Fig. II-1. Profiles of stability parameters for 50mb layers from 900-200mb and 25mb layers from 200-100mb. Layer stabilities are scaled with respect to values in lowest layer (900-850mb). Profiles are averaged over the 30 U.S. radiosonde stations whose surface pressure remains above 900mb. Each station profile is the average of 10 Januarys, 1946-55 (see Gates (1961) for analyses of additional stability parameters for a slightly different data set).

continuity equation. All other notations are defined in the conventional manner.

The measure of the stability term $\frac{\partial P}{\partial \theta}$ in Eq. (II-6) can be expressed in terms of M such that

$$\ell n\left(\frac{\partial P}{\partial \theta}\right) = \ell n\left[C\left(\frac{\partial M}{\partial \theta}\right)^{C_v/R} \left(\frac{\partial^2 M}{\partial \theta^2}\right)\right]$$

$$C = Poo/RC_p^{C_v/R}, \quad Poo = 1000 \text{ mb}$$

This equation may be obtained by combining Eqs. (II-3) and (II-5), but the relationship between p and M is highly nonlinear. To avoid the complexity, we introduce the so-called "Boussinesq approximation" into the mass continuity equation (II-6), which yields

$$\frac{\partial}{\partial t}\left(\frac{\partial z}{\partial \theta}\right) + u\frac{\partial}{\partial x}\left(\frac{\partial z}{\partial \theta}\right) + v\frac{\partial}{\partial y}\left(\frac{\partial z}{\partial \theta}\right) + \left(\frac{\partial z}{\partial \theta}\right)\left(\frac{\partial u}{\partial x} + \frac{\partial v}{\partial y}\right) = 0 \qquad \text{(II-7)}$$

This Boussinesq-approximated continuity Eq. (II-7) differs from Eq. (II-6) in that z replaces p.

Using the definition of Montgomery stream function Eq. (II-4), the hydrostatic relationship (II-3) becomes

$$M - \theta\frac{\partial M}{\partial \theta} = gz \qquad \text{(II-8)}$$

The horizontal equations of motion (Eqs. (II-1) and (II-2)), the Boussinesq-approximated mass continuity equation (II-7) and the hydrostatic relationship (II-8) then comprise a closed set of equations with four unknown, dependent variables u, v, M and z.

To investigate the secondary circulations set up in the free atmosphere by boundary forcing, it is convenient to introduce a linear

perturbation method which always retains the underlying local geometrical properties of the original system. Suppose all variables consist of mean and superimposed small perturbations according to

$$\begin{aligned} u(x,y,\theta,t) &= \bar{U} + u'(x,y,\theta,t) \\ v(x,y,\theta,t) &= v'(x,y,\theta,t) \\ M(x,y,\theta,t) &= \bar{M}(y,\theta) + M'(x,y,\theta,t) \\ z(x,y,\theta,t) &= \bar{z}(\theta) + z'(x,y,\theta,t) \end{aligned} \qquad \text{(II-9)}$$

where bar quantities represent the basic state and the prime quantities are small perturbations superimposed on the mean values. Furthermore, we assume the basic flow field is a constant zonal current $\bar{U}$=const., in which case the basic equations are simplified. Substituting Eq. (II-9) into Eqs. (II-1), (II-2), (II-8) and (II-7), we obtain for the basic equations

$$\frac{\partial \bar{M}}{\partial x} = 0 \qquad \text{(II-10-a)}$$

$$f\bar{U} = -\frac{\partial \bar{M}}{\partial y} = \text{const.} \qquad \text{(II-10-b)}$$

$$\bar{M} - \theta\frac{\partial \bar{M}}{\partial \theta} = g\bar{z} \qquad \text{(II-10-c)}$$

$$\frac{\partial}{\partial t}\left(\frac{\partial \bar{z}}{\partial \theta}\right) + \bar{U}\frac{\partial}{\partial x}\left(\frac{\partial \bar{z}}{\partial \theta}\right) = 0 \qquad \text{(II-10-d)}$$

and for the perturbation equations

$$\frac{\partial u'}{\partial t} + \bar{U}\frac{\partial u'}{\partial x} - fv' = -\frac{\partial M'}{\partial x} \qquad \text{(II-11-a)}$$

$$\frac{\partial v'}{\partial t} + \bar{U}\frac{\partial v'}{\partial x} + fu' = -\frac{\partial M'}{\partial y} \qquad \text{(II-11-b)}$$

$$M' - \theta\frac{\partial M'}{\partial \theta} = gz' \qquad \text{(II-11-c)}$$

$$\frac{\partial}{\partial t}\left(\frac{\partial z'}{\partial \theta}\right) + \bar{U}\frac{\partial}{\partial x}\left(\frac{\partial z'}{\partial \theta}\right) + u'\frac{\partial}{\partial x}\left(\frac{\partial \bar{z}}{\partial \theta}\right) + v'\frac{\partial}{\partial y}\left(\frac{\partial \bar{z}}{\partial \theta}\right) + \frac{\partial \bar{z}}{\partial \theta}\left(\frac{\partial u'}{\partial x} + \frac{\partial v'}{\partial y}\right) = 0 \qquad \text{(II-11-d)}$$

where the products of perturbations are neglected. The basic flow is geostrophic Eqs. (II-10-a) and (II-10-b), and hydrostatic Eq. (II-10-c). Eq. (II-10-d) implies that the basic stability $\frac{\partial \bar{z}}{\partial \theta}$ is time independent, since the second term of Eq. (II-10-d) is identically zero. This can be shown by operating on Eq. (II-10-c) with $\frac{\partial^2}{\partial \theta \partial x}$ and recalling that the basic flow is constant.

Then

$$\left(\frac{\partial \bar{z}}{\partial \theta}\right) = \left(\frac{\partial \bar{z}}{\partial \theta}\right)_{t=0}$$

and $\frac{\partial}{\partial x}\left(\frac{\partial \bar{z}}{\partial \theta}\right)$ and $\frac{\partial}{\partial y}\left(\frac{\partial \bar{z}}{\partial \theta}\right)$ of Eq. (II-11-d) vanish. Once again utilizing the Poisson's equation (II-5), we can represent $\frac{\partial \bar{z}}{\partial \theta}$ in terms of basic stability such that

$$\frac{\partial \bar{z}}{\partial \theta} = \frac{\bar{T}}{\theta}\Big/\left(\Gamma_d - \gamma\right) = \frac{gN^{-2}}{\theta} \qquad \text{(II-12)}$$

where Γ_d is the dry adiabatic lapse rate, $\gamma = -\frac{\partial \bar{T}}{\partial z}$, and $N = \left(\frac{\bar{T}}{g(\Gamma_d - \gamma)}\right)^{-\frac{1}{2}}$ is Brunt-Väisälä frequency.

To estimate the importance of various terms, we scale the variables as follows:

$$(x,y) = L(\hat{x},\hat{y})$$

$$t = \tau\hat{t}$$

$$(u',v') = \bar{U}(\hat{u},\hat{v}) \qquad \text{(II-13)}$$

$$M' = fL\bar{U}\hat{M}$$

$$z' = \frac{\theta_o f L \bar{U}}{g\Delta\theta}\hat{z} \qquad \text{(II-13 cont'd)}$$

$$\theta = \theta_o + \Delta\theta\hat{\theta}$$

where L is a forcing length scale, τ is the spin-down time scale to be determined later, and $\bar{U}$ is a typical velocity scale. The choice of the scale of M' is obtained by expecting a rough balance between the Coriolis force and the pressure gradient force, and obtaining z' from hydrostatic balance. θ_o and $\Delta\theta$ represent, respectively, the potential temperature at the bottom of the free atmosphere and the potential temperature thickness of the free atmosphere influenced by boundary pumping, which will be determined later.

Substituting Eq. (II-13) into Eq. (II-11-a) through Eq. (II-11-d) yields

$$\lambda\frac{\partial\hat{u}}{\partial\hat{t}} + R_o\frac{\partial\hat{u}}{\partial\hat{x}} - \hat{v} = -\frac{\partial\hat{M}}{\partial\hat{x}} \qquad \text{(II-14-a)}$$

$$\lambda\frac{\partial\hat{v}}{\partial\hat{t}} + R_o\frac{\partial\hat{v}}{\partial\hat{x}} + \hat{u} = -\frac{\partial\hat{M}}{\partial\hat{y}} \qquad \text{(II-14-b)}$$

$$\frac{\partial\hat{z}}{\partial\hat{\theta}} = -\left(1 + \frac{\Delta\theta}{\theta_o}\hat{\theta}\right)\frac{\partial^2\hat{M}}{\partial\hat{\theta}^2} \qquad \text{(II-14-c)}$$

$$\lambda\frac{\partial}{\partial\hat{t}}\left(\frac{\partial\hat{z}}{\partial\hat{\theta}}\right) + R_o\frac{\partial}{\partial\hat{x}}\left(\frac{\partial\hat{z}}{\partial\hat{\theta}}\right) + \frac{B^{-2}}{\left(1+\frac{\Delta\theta}{\theta_o}\hat{\theta}\right)}\left(\frac{\partial\hat{u}}{\partial\hat{x}} + \frac{\partial\hat{v}}{\partial\hat{y}}\right) = 0 \qquad \text{(II-14-d)}$$

where

$$\lambda \equiv \frac{1}{f\tau}$$

$$R_o \equiv \frac{\bar{U}}{fL}$$

$$B \equiv \frac{NfL\theta_o}{g\Delta\theta}$$

$$N \equiv \left(\frac{g}{\theta}\ \frac{\partial\theta}{\partial\bar{z}}\right)^{\frac{1}{2}}$$

The interpretation of the stability parameter B is facilitated by using the definition of Brunt-Väisälä frequency and momentarily setting $\theta = \theta_o$ (homogeneous atmosphere), in which case we obtain

$$B = \frac{fL}{g'}\left(\frac{g}{\theta_o}\frac{\partial\theta}{\partial\bar{z}}\right)^{\frac{1}{2}} \simeq L\left(\frac{f^2}{g'H}\right)^{\frac{1}{2}} \equiv \frac{L}{L_R}$$

where $g' = \frac{\Delta\theta}{\theta_o}g$, H is the fluid depth and $L_R \equiv \frac{\sqrt{g'H}}{f}$ is the Rossby radius of deformation. For mid-latitude synoptic-scale motions, B is generally O(1). As a numerical example, for g=10 m sec^{-2}, $\Delta\theta = 30^oK$, $\theta_o = 280^oK$, $\frac{\partial\theta}{\partial\bar{z}} = 4 \times 10^{-3}\ ^oK\ m^{-1}$, $L = 10^6$ m and $f = 10^{-4}$ sec^{-1}, then $N^{-1} \simeq 80$ sec and $B \simeq 1$. The parameter B defined in isentropic coordinates differs from that defined in Cartesian coordinates (see Walin, 1969) since $\frac{\partial\bar{z}}{\partial\theta}$ varies inversely with temperature.

We now impose restrictions on values of the parameters that appear in the above equations. This allows us to conveniently examine special problems in which we are interested. In the intermediate stage of the spin-down process, it is possible to assume that the dimensional time scale τ is large compared with the Coriolis force time scale f^{-1}, but still small compared with the turbulent diffusion time scale in the free atmosphere, i.e. $E<<\lambda<<1$ where E is the turbulent Ekman number. It has also been assumed that advections by the mean flow are small compared with the local changes induced by boundary pumping, i.e. $\lambda>>R_o$. This implies that the basic flow is sufficiently weak or the length

scale is sufficiently large. As long as we are concerned with the role of stratification, it is natural to assume that B is at least of order unity. Evaluation of B indicates that it is typically O(1) for tropospheric synoptic-scale flow. The parameter λ is expected to be small since quasi-geostrophic adjustments are expected to be slow. Taking advantage of this small parameter, we expand the dependent variables in terms of a power series in λ as in Holton (1965) and Walin (1969). The zero-and first-order equations are then

$$-v_o = -\frac{\partial M_o}{\partial x} \qquad \text{(II-15-a)}$$

$$u_o = -\frac{\partial M_o}{\partial y} \qquad \text{(II-15-b)}$$

$$\frac{\partial z_o}{\partial \theta} = -\left(1 + \frac{\Delta\theta}{\theta_o}\theta\right)\frac{\partial^2 M_o}{\partial \theta^2} \qquad \text{(II-15-c)}$$

$$\frac{B^{-2}}{1+\frac{\Delta\theta}{\theta_o}\theta}\left(\frac{\partial u_o}{\partial x} + \frac{\partial v_o}{\partial y}\right) = 0 \qquad \text{(II-15-d)}$$

and

$$\frac{\partial u_o}{\partial t} - v_1 = -\frac{\partial M_1}{\partial x} \qquad \text{(II-16-a)}$$

$$\frac{\partial v_o}{\partial t} + u_1 = -\frac{\partial M_1}{\partial y} \qquad \text{(II-16-b)}$$

$$\frac{\partial z_1}{\partial \theta} = -\left(1 + \frac{\Delta\theta}{\theta_o}\theta\right)\frac{\partial^2 M_1}{\partial \theta^2} \qquad \text{(II-16-c)}$$

$$\frac{\partial}{\partial t}\left(\frac{\partial z_o}{\partial \theta}\right) + \frac{B^{-2}}{1+\frac{\Delta\theta}{\theta_o}\theta}\left(\frac{\partial u_1}{\partial x} + \frac{\partial v_1}{\partial y}\right) = 0 \qquad \text{(II-16-d)}$$

where we drop the "^" notation and the subscript is the expansion index.

To O(1) the flow is geostrophic, hydrostatic and non-divergent. Equations of $O(\lambda)$ are time dependent. Combining the first-order equations (II-16-a), (II-16-b) and (II-16-d) and using equations (II-15-a)-(II-15-c), we get a single conservation equation for the zero order potential vorticity

$$\frac{\partial}{\partial t}\left[\frac{\partial^2 M_o}{\partial x^2}+\frac{\partial^2 M_o}{\partial y^2}+B^2\left(1+\frac{\Delta\theta}{\theta_o}\theta\right)^2\frac{\partial^2 M_o}{\partial \theta^2}\right]=0 \qquad \text{(II-17)}$$

Eq. (II-17) is a linearized version of the quasi-geostrophic potential vorticity equation (e.g., Phillips, 1963; Charney and Stern, 1962). The Boussinesq assumption gives us a simpler form of the potential vorticity equation than the one considered by Bleck (1973) for numerical analysis.

We observe that if M_o is known, the zero-order fields (u_o, v_o, z_o) are completely determined by Eq. (II-15) and the initial distribution of these variables. We now examine the development in time of the zero-order fields.

Let us first examine the boundary conditions in order to solve the elliptic equation for $\frac{\partial M_o}{\partial t}$ (Eq. (II-17)) as an initial value problem. We require the specification of M_o at the bottom and top of the free atmosphere, together with side and upstream boundary conditions. We will consider a simple harmonic x and y dependency in the form of $\mathrm{Re}\left\{e^{i(kx+ly)}\right\}$, where $\mathrm{Re}\{X\}$ represents the real part of function X. In this manner we may impose the horizontal forcing length scale explicitly. The required boundary condition at the bottom of the free atmosphere may be obtained from Eq. (II-11-c). Taking the total derivative

$$\frac{d}{dt}\left(M'-\theta\frac{\partial M'}{\partial\theta}\right) = g\frac{dz'}{dt} \qquad \text{at} \quad \theta=\theta_o \qquad \text{(II-18)}$$

At the bottom boundary, the total change of the perturbed stream function on an isentropic surface is due to the perturbed temperature and geopotential height changes. The height change of the constant θ surface at the bottom of the free atmosphere may be caused by irregular terrain features and/or boundary layer pumping. At present, we assume a flat surface so that the height change of the θ surface is due only to the Ekman pumping. The quasi-geostrophic theory allows the parameterization of $\left.\frac{dz'}{dt}\right|_{\theta=\theta_o}$ in terms of M' only

$$\left.\frac{dz'}{dt}\right|_{\theta=\theta_o} = F\zeta_g = \frac{F}{f}\left(\frac{\partial^2 M'}{\partial x^2}+\frac{\partial^2 M'}{\partial y^2}\right) \quad \text{at } \theta=\theta_o \qquad \text{(II-19)}$$

where F is the Ekman pumping efficiency and ζ_g is the geostrophic vorticity. In the case of Ekman flow with constant eddy viscosity K (Charney and Eliassen, 1949)

$$F \simeq \sin 2\hat{\alpha}\left(\frac{K}{2f}\right)^{1/2}$$

where $\hat{\alpha}$ is the angle between surface geostrophic and actual wind. In the case of a turbulent boundary layer parameterized in terms of a drag law (Mahrt, 1974),

$$F \simeq \frac{\hat{C}_D h}{1+\hat{C}_D^2}, \qquad \hat{C}_D = \frac{C_D\overline{U}}{fh}$$

where C_D is a surface drag coefficient and h is the boundary layer depth. F may vary substantially for the stratified boundary layer, since K and $\hat{\alpha}$ depend on the stratification in the first case while C_D and h vary with

the stratification in the second case. The influence of stratification on the boundary layer pumping is examined more closely in section III. For now we assume F to be constant.

Combining Eqs. (II-18) and (II-19), scaling according to Eq. (II-13), letting $R_o \to 0$, and rearranging, we obtain

$$\lambda \frac{\partial}{\partial t}\left[\frac{\Delta\theta}{\theta_o} M - \left(1+\frac{\Delta\theta}{\theta_o}\theta\right)\frac{\partial M}{\partial \theta}\right] = \frac{gF}{f^2L^2}\frac{\Delta\theta}{\theta_o}\left(\frac{\partial^2 M}{\partial x^2} + \frac{\partial^2 M}{\partial y^2}\right) \quad \text{at } \theta = 0 \quad \text{(II-20)}$$

where we again drop the "^" notations. Since $\frac{\Delta\theta}{\theta_o} << 1$ for atmospheric problems, the primary balance is

$$-\lambda \frac{\partial}{\partial t}\left(\frac{\partial M}{\partial \theta}\right) = \frac{gF}{f^2L^2}\frac{\Delta\theta}{\theta_o}\left(\frac{\partial^2 M}{\partial x^2} + \frac{\partial^2 M}{\partial y^2}\right)$$

Considering time changes to be driven by the Ekman pumping suggests the choice,

$$\lambda = \frac{gF}{f^2L^2}\frac{\Delta\theta}{\theta_o} \qquad \text{or} \qquad \tau = \frac{fL^2\theta_o}{gF\Delta\theta}$$

This may be interpreted as the spin-down time scale of the barotropic atmosphere. Choosing this time scale to be the scaling time scale and expanding the flow in terms of powers of λ, as above, we obtain the zero-order bottom boundary conditions:

$$\frac{\partial}{\partial t}\left[\frac{\Delta\theta}{\theta_o} M_o - \left(1+\frac{\Delta\theta}{\theta_o}\theta\right)\frac{\partial M_o}{\partial \theta}\right] = \frac{\partial^2 M_o}{\partial x^2} + \frac{\partial^2 M_o}{\partial y^2} \qquad \text{(II-21)}$$

The top boundary condition is the assumption that the perturbation quantities vanish as $\theta \to$ large.

$$M_o \to 0 \qquad \text{as} \qquad \theta \to \text{large} \qquad \text{(II-22)}$$

B. The Solution with Horizontal Harmonic Forcing

For mathematical convenience, we introduce a new variable η which is defined by

$$\eta = \ell n \left(1+\frac{\Delta\theta}{\theta_o}\,\theta\right) \tag{II-23}$$

Substituting Eq. (II-23) into Eqs. (II-17), (II-21) and (II-22), we get

$$\frac{\partial}{\partial t}\left[\frac{\partial^2 M_o}{\partial x^2} + \frac{\partial^2 M_o}{\partial y^2} + \left(\frac{NfL}{g}\right)^2 \left(\frac{\partial^2 M_o}{\partial \eta^2} - \frac{\partial M_o}{\partial \eta}\right)\right] = 0 \tag{II-24}$$

$$\frac{\partial}{\partial t}\left(M_o - \frac{\partial M_o}{\partial \eta}\right) = \frac{\theta_o}{\Delta\theta}\left(\frac{\partial^2 M_o}{\partial x^2} + \frac{\partial^2 M_o}{\partial y^2}\right) \quad \text{at } \eta = 0 \tag{II-25}$$

$$M_o \to 0 \qquad \text{as } \eta \to \text{large} \tag{II-26}$$

Now $M_o = M_o(x,y,\eta,t)$, so it will obviously be necessary to separate out the horizontal dependence to solve (II-24), subject to boundary conditions (II-25) and (II-26). We now assume the harmonic horizontal dependency, in which case the solution of Eq. (II-24) can be written as

$$M_o(x,y,\eta,t) = \hat{m}(\eta,t)\ \ \mathrm{Re}\left\{\exp(i(kx+\ell y))\right\}$$

From Eqs. (II-24), (II-25) and (II-26), we obtain the following governing equation and boundary conditions for $\hat{m}(\eta,t,k,\ell)$

$$\frac{\partial}{\partial t}\left[-\hbar^2\hat{m}(\eta,t) + \left(\frac{NfL}{g}\right)^2 \left(\frac{\partial^2 \hat{m}}{\partial \eta^2} - \frac{\partial \hat{m}}{\partial \eta}\right)\right] = 0 \tag{II-27}$$

$$\frac{\partial}{\partial t}\left(\hat{m} - \frac{\partial \hat{m}}{\partial \eta}\right) = -\frac{\theta_o}{\Delta\theta}\hbar^2\hat{m} \qquad \text{at} \quad \eta = 0 \tag{II-28}$$

$$\hat{m} \to 0 \qquad \text{as} \quad \eta \to \text{large} \tag{II-29}$$

where $\hbar^2 = k^2 + \ell^2$

We now separate the time dependence in Eqs. (II-27), (II-28) and (II-29) by applying the Laplace transform

$$m(\eta,p) = \int_0^\infty \hat{m}(\eta,t)e^{-pt}\,dt$$

Eqs. (II-27) and (II-28) are converted to ordinary differential equations in η with constant coefficients. The solution is

$$m(\eta;p,\ell) = \left(-\frac{2\frac{\theta_o}{\Delta\theta}\ell^2\,\hat{m}(0,0)}{1+\alpha}\right)\frac{e^{\frac{1-\alpha}{2}\eta}}{p\left(p+\frac{2\frac{\theta_o}{\Delta\theta}\ell^2}{1+\alpha}\right)} + \frac{\hat{m}(\eta,0)}{p} \qquad \text{(II-30)}$$

where

$$\alpha = \left[1+\left(\frac{2\ell g}{fLN}\right)^2\right]^{\frac{1}{2}}$$

Applying the inverse Laplace transform $\hat{m}(\eta,t) = \frac{1}{2\pi C}\int_{A-i\infty}^{A+i\infty} m(\eta,p)e^{pt}dp$ to Eq. (II-30), where the constant A has been chosen so that all the singularities of Eq. (II-30) are on the right half-plane, and using the residue theorem, we obtain the final solution

$$M_o(x,y,\eta,t;k,\ell) = \left[\hat{m}(\eta,0)-\left\{\hat{m}(0,0)\left(1-e^{-\frac{2\frac{\theta_o}{\Delta\theta}\ell^2}{1+\alpha}t}\right)\right\}\cdot e^{\frac{1-\alpha}{2}\eta}\right]\mathrm{Re}\left\{e^{i(kx+\ell y)}\right\} \qquad \text{(II-31)}$$

The associated fields (u_o, v_o, z_o) are also obtained by Eq. (II-15a,b,c) with Eq. (II-31). The dimensional form of Eq. (II-31) is,

$$M_o(x,y,\theta,t;\ell) = \left[\hat{m}(\theta,0)-\left\{\hat{m}(0,0)\left(1-e^{-\frac{t}{t_e}}\right)\right\}\left(\frac{\theta}{\theta_o}\right)^{\frac{1-\alpha'}{2}}\right]\cdot \mathrm{Re}\left\{e^{i(kx+\ell y)}\right\} \qquad \text{(II-32)}$$

where

$$t_e = \frac{f(1+\alpha')}{2g\ell h^2} \qquad \text{(II-33)}$$

$$\alpha' = \left[1 + \left(\frac{2g\ell h}{fN}\right)^2\right]^{\frac{1}{2}}$$

We first note that the amplitude of the flow does not change with time in the absence of boundary layer pumping, i.e., when F=0. The initial imposed perturbation remains stationary. With boundary layer pumping, the spin-down scale t_e decreases with increasing stratification. If we define the potential temperature θ_e at the penetration depth where the vorticity destruction rate is reduced to e^{-1} of its value near the bottom of the free atmosphere, the penetration potential temperature thickness is

$$\delta\theta = \theta_e - \theta_o = \theta_o\left[\exp\left(\frac{2}{\alpha'-1}\right) - 1\right]$$

Since $\delta\theta = \frac{\partial\theta}{\partial z}\,\delta z \simeq \frac{\theta_o}{g} N^2 \delta z$, where δz represents the penetration depth, we can estimate the penetration depth scale δz to be

$$\delta z = \frac{g}{N^2}\left[\exp\left(\frac{2}{\alpha'-1}\right) - 1\right]$$

For mid-latitude synoptic-scale flows, $\frac{2g\ell h}{fN} >> 1$. For example, for $f=10^{-4}\text{sec}^{-1}$, $N^{-1} = 80$ sec and $L = 2\times10^6\text{m} = \frac{2\pi}{\ell}$ then

$$\frac{2g\ell h}{fN} = 50$$

In this case the spin-down time scale t_e and the penetration depth scale δz are approximately

$$t_e \simeq \frac{\ell h^{-1}}{FN} \qquad \text{(II-35)}$$

$$\delta z = \frac{g}{N^2}\left(e^{\frac{fN}{gh}} - 1\right) \simeq \frac{f}{Nh} \qquad \text{(II-35)}$$

The penetration depth scale defined in Eq. (II-35) is the natural vertical scale of the stratified free flow which responds to any perturbation whose horizontal length scale is "L". This natural vertical scale is often called the Lineykin layer (Lineykin, 1955). With increasing stratification, the spin-down time scale t_e and the penetration depth scale δz decrease. This is because the circulation induced by the boundary layer pumping is increasingly bottom trapped with increasing stratification, thus increasing the divergence and the rate of pressure adjustment immediately above the boundary layer. We also note that the greater the horizontal length scale, the greater the time required for a parcel following the frictionally-driven secondary circulation to complete one cycle. If the imposed horizontal length scale is very large, so that the spin-down time scale t_e is comparable to $\frac{f}{gFh^2}$, the effect of stratification on the penetration depth scale is no longer relevant, and the atmosphere responds like a homogeneous atmosphere.

In Figs. II-2 and II-3 the perturbed relative vorticity profiles are plotted versus time and potential temperature, respectively, for typical values of the parameters and the initial condition $\hat{m}(\theta,0) = \hat{m}(0,0)$. The influence of Ekman pumping is more significant in the lower atmosphere than in the higher atmosphere. Near the bottom (Fig. II-2) the fluid has spun down for three days, while far above the bottom the fluid is still not affected by boundary layer pumping. Thus, the spin-down time scale for the stratified atmosphere differs from level to

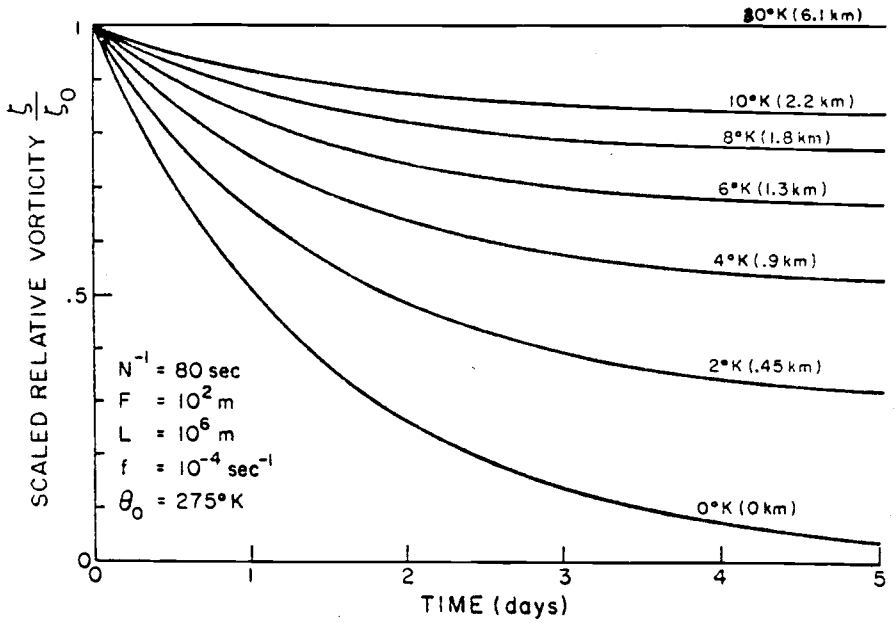

Fig. II-2. Spin-down of relative vorticity (scaled with respect to the height-independent initial value) at different levels in the free flow. Plots are labeled according to their potential temperature excess and elevation above the boundary layer top.

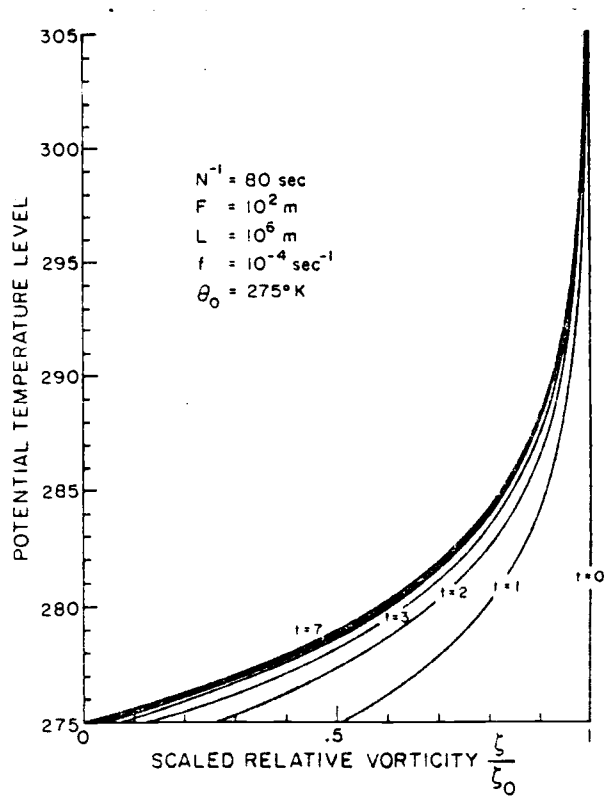

Fig. II-3. Spin-down of scaled relative vorticity. Plots are labeled according to number of days after initiation of spin-down.

level as mentioned in Sec. I. It is evident from Figs. II-2 and II-3 that boundary layer pumping can significantly alter synoptic-scale motion in the lower troposphere.

C. Free Flow Response to Diurnally-Varying Boundary Layer Pumping

In developing the above spin-down problem, a constant pumping efficiency has been employed, since a more realistic parameterization of Ekman pumping efficiency F is quite difficult. Assuming that F is constant implies that the eddy exchange coefficient or drag coefficient is constant for all time and that the boundary layer thickness is also constant. In the real atmosphere neither of these assumptions is true. In this section, following Buajitti and Blackadar (1957), Estoque (1963), and Krishna (1968), we assume that the Ekman pumping efficiency has a diurnal variation of the form

$$F = \overline{F}\,(1 + \varepsilon \cos \Omega t) \tag{II-36}$$

where $\overline{F}$ is the time-mean Ekman pumping efficiency, ε is the diurnal amplitude divided by the time-mean Ekman pumping efficiency, assumed small enough to be applicable to the perturbation theory, and Ω is the diurnal frequency. With this simple parameterization of Ekman pumping efficiency, we employ the method used above to obtain the dimensionless solution

$$M_o(x,y,\eta,t;\ell h,\Omega) = \left[\hat{m}(\eta,0) - \hat{m}(0,0)e^{\frac{1-\alpha}{2}\eta}\right]\left\{\frac{1}{1+\varepsilon}\left(1-e^{-\frac{2\beta\ell^2h^2(1+\varepsilon)}{1+\alpha}t}\right) - \right.$$

$$\left.\frac{2\beta\ell^4h^4\varepsilon(1+\varepsilon)}{4\beta^2\ell^4h^4(1+\varepsilon)^2+\omega^2(1+\alpha)^2}\cdot\exp\left(-\frac{2\beta\ell^2h^2(1+\varepsilon)}{1+\alpha}t\right) + \frac{\beta\ell^2h^2\varepsilon}{4\beta^2\ell^4h^4(1+\varepsilon)^2+\omega^2(1+\alpha)^2}\cdot\right.$$

$$(2\beta\ell^2(1+\varepsilon)\cos\ \omega t-2\omega(1+\varepsilon)\sin\ \omega t)\Big\}\Big]\ \mathrm{Re}\left[\exp\left\{i(kx+\ell y)\right\}\right]$$

where $\beta = \frac{\theta_o}{\Delta\theta}$, $\alpha = \left[1+\left(\frac{2g\ell}{fLN}\right)^2\right]^{\frac{1}{2}}$, $\omega = \Omega\tau$

To facilitate interpretation of the above solution, we consider a weak diurnal variation, i.e. $\varepsilon<<1$. Noting that $\Omega<<N$ and $\alpha\simeq\frac{2g\ell}{fLN}$ for synoptic-scale motion, and expanding in terms of ε, we obtain the dimensional form of the solution

$$M_o(x,y,\theta,t;h)=\mathrm{Re}\left[\exp\left\{i(kx+\ell y)\right\}\right]\cdot\left[\hat{m}(\theta,0)-\hat{m}(0,0)\left(\frac{\theta}{\theta_o}\right)^{\frac{1-\alpha'}{2}}\cdot\right.$$
$$\left.\left\{\left(1-e^{-\frac{t}{\bar{t}_e}}\right)-\varepsilon\left(1-\frac{t}{\bar{t}_e}e^{-\frac{t}{\bar{t}_e}}-\cos\Omega t\right)+O(\varepsilon^2)\right\}\right] \qquad \text{(II-37)}$$

where $\bar{t}_e = \frac{N^{-1}}{\bar{F}\ell}$

The first term of the inner bracket of Eq. (II-37) is the spin-down solution for the time-mean Ekman efficiency (see Eq. (II-32)) and the second term of the inner bracket (ε term) represents the diurnal effects, consisting of a slowly-damping term and a diurnal oscillation. The diurnal oscillation does not vanish as time approaches infinity because of the oscillating pressure field caused by the diurnal Ekman pumping.

The spin-down time scale given by $\bar{t}_e$ is essentially the same as in Eq. (II-35), except that $\bar{F}$ replaces F. The penetration depth scale of the frictional effect is not affected by the diurnal oscillation of the Ekman pumping efficiency at least to lowest order. This scale is once again proven to be a natural property of the stratified fluid. This decay of the diurnal oscillation with height is evident in Fig. II-4.

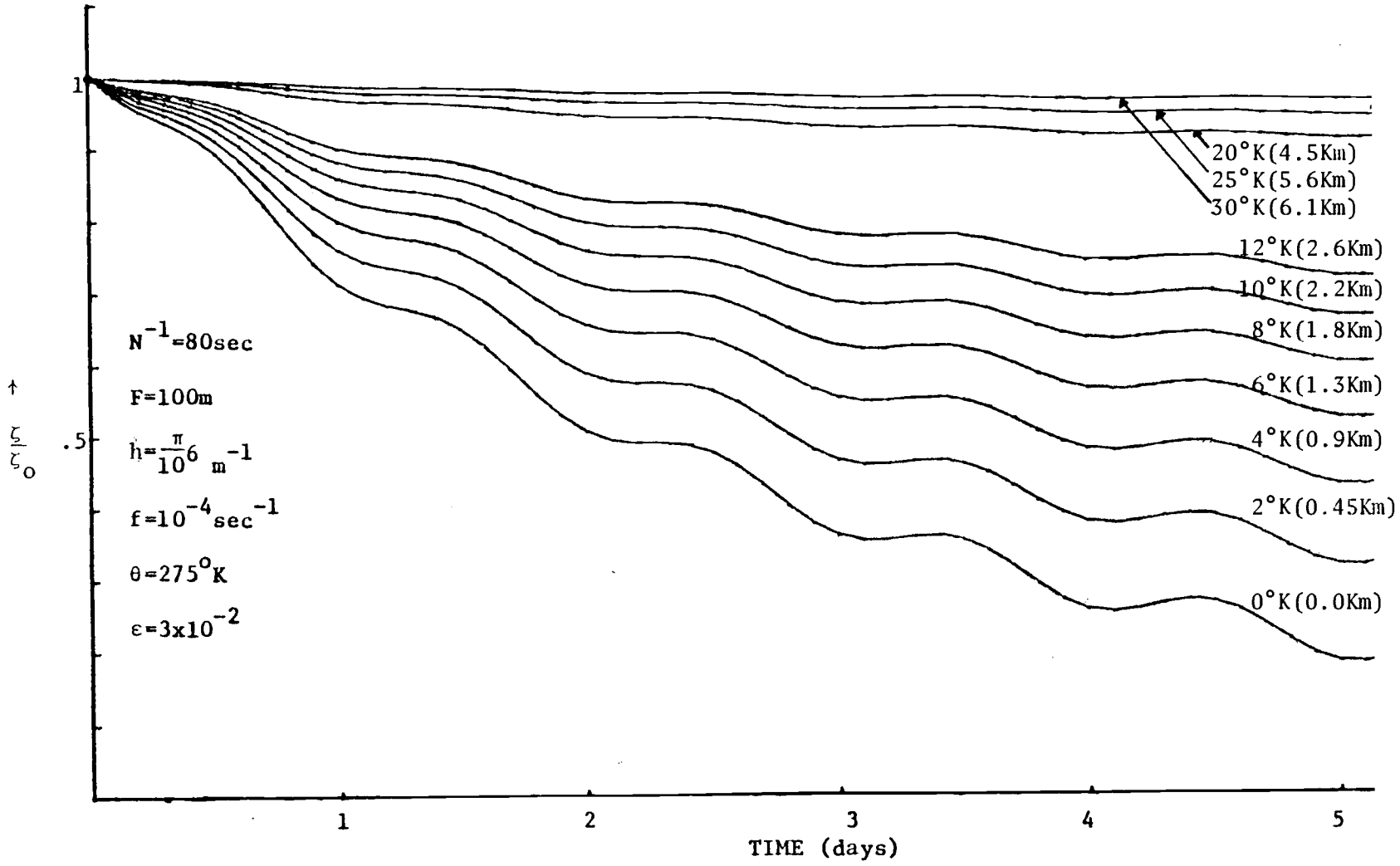

Fig. II-4. As in Fig. II-2 except the diurnally-varying pumping efficiency.

III. TIME OSCILLATING STRATIFIED BOUNDARY LAYER

Many investigators have studied either oscillating boundary layers or stratified boundary layers. In geophysical flows, however, such effects occur simultaneously with important interactions. Kuo (1973) has considered such interactions analytically. By considering certain simplifications to Kuo's system, the present analysis clarifies some of the physics of such interactions and extends the analysis to a wider range of oscillation frequencies.

Various layers in the oscillating boundary layer experience phase shifts with respect to both the forcing stimulus and to each other, and the amplitudes of the response decrease away from the boundary. These phase shifts and amplitude decays are a consequence of the viscosity of the fluid (Lighthill, 1954; Kestin et. al., 1960).

In this section we study boundary layers which are forced by a weak time-dependent surface temperature perturbation with spatial variation in amplitude. In geophysical flows, such variations in surface temperature could be associated with horizontal variations in surface properties such as heat capacity, as occur in the sea breeze and urban heat island problems. The study of Stommel and Veronis (1957) belongs to the limiting case of this study (i.e. $\hat{\omega}\to 0$, where $\hat{\omega}$ is the nondimensional forcing frequency). However, their solutions are not quite completed because of the arbitrariness of the geostrophic wind used. We will investigate the unsteady solutions for the parameter region $\hat{\omega}<1$ and $m<<1$, where m is the product of a stratification parameter B^2 and Ekman number E. However, we will not consider the case of resonance frequency (i.e. $\hat{\omega}=1$) considered by several authors (Mak, 1974; Kuo,

1975; Cogley, 1976; Bergstrom and Cogley, 1976).

A. Governing Equations

We assume the field variables to be independent of the y-direction, i.e. $\frac{\partial(\ )}{\partial y} = 0$ and periodic with time, as for example, in Holton (1967), such that

$$q(x,y,z,t) = \hat{q}(x,z)e^{-it} \tag{III-1}$$

where q represents any field variable. We introduce a stretched vertical coordinate $\eta=\frac{z}{\delta}$, where δ is the thickness of the boundary layer and further assume the field variables are periodically dependent on x, as for example, in Stommel and Veronis (1957), Leetmaa (1971), Hsueh and Kenney (1972), and Kuo (1973) in which case

$$\begin{aligned}(\tilde{u},\tilde{v}) &= (u'(\eta),v'(\eta))\sin x \\ (\tilde{p},\tilde{\theta},\tilde{w}) &= (p'(\eta),\theta'(\eta),w'(\eta))\cos x\end{aligned} \tag{III-2}$$

Substituting Eqs. (III-1) and (III-2) into Eqs. (A-II-10) through (A-II-14) (see Appendix II), we find

$$-i\hat{\omega}u' - v' = p' + \frac{E}{\delta^2}\frac{d^2u'}{d\eta^2} \tag{III-3-a}$$

$$-i\hat{\omega}v' + u' = \frac{E}{\delta^2}\frac{d^2v'}{d\eta^2} \tag{III-3-b}$$

$$\frac{dP'}{d\eta} = \delta\theta' \tag{III-3-c}$$

$$-i\hat{\omega}\theta' + B^2w' = \frac{E}{\delta^2}\frac{d^2\theta'}{d\eta^2} \tag{III-3-d}$$

$$\delta u' + \frac{dw'}{d\eta} = 0 \qquad \text{(III-3-e)}$$

As discussed in Appendix III we explicitly neglect the Newtonian radiational effect in contrast to Holton (1967) and Blumsack et. al. (1973). This system is similar to that examined by Kuo (1973) except here f is assumed constant.

B. Possible Types of Natural Boundary Layers

Combining Eqs. (III-3,a-e) we obtain an equation for p'

$$\left(\frac{E}{\delta^2}\frac{d^2}{d\eta^2} + i\hat{\omega}\right)\left(\frac{d^6}{d\eta^6} + \frac{2\hat{\omega}\delta^2}{E}\, i\, \frac{d^4}{d\eta^4} + \frac{(1-\hat{\omega}^2)\delta^4}{E^2}\, \frac{d^2}{d\eta^2} - \frac{B^2\delta^6}{E^2}\right)p' = 0 \qquad \text{(III-4)}$$

The factor $\left(\frac{E}{\delta^2}\frac{d^2}{d\eta^2} + i\hat{\omega}\right)p'$ represents the thermal Stokes oscillating boundary layer with frequency ω and dimensional boundary layer thickness $\left(\frac{2K}{\omega}\right)^{\frac{1}{2}}$. This layer is associated with temperature diffusion.

We first consider the possible two-term balances (as in Blumsack and Barcilon (1971)) in the second parenthesis in Eq. (III-4). The restriction that the remaining terms be small compared with those retained allows us to form relationships among the governing parameters, B^2, E, and $\hat{\omega}$ for each region of parameter space depicted in Fig. III-1. Subdivision of region II in Fig. III-1 is facilitated by altering the principal balance in thermodynamic equation III-3-d, which in turn depends upon the relative magnitude of the local acceleration and diffusion terms.

The six possible two-term balances are summarized in Table 1. In the atmosphere any one of the boundary layers listed in Table 1 may occur in nearly pure form or in combination with the other types of

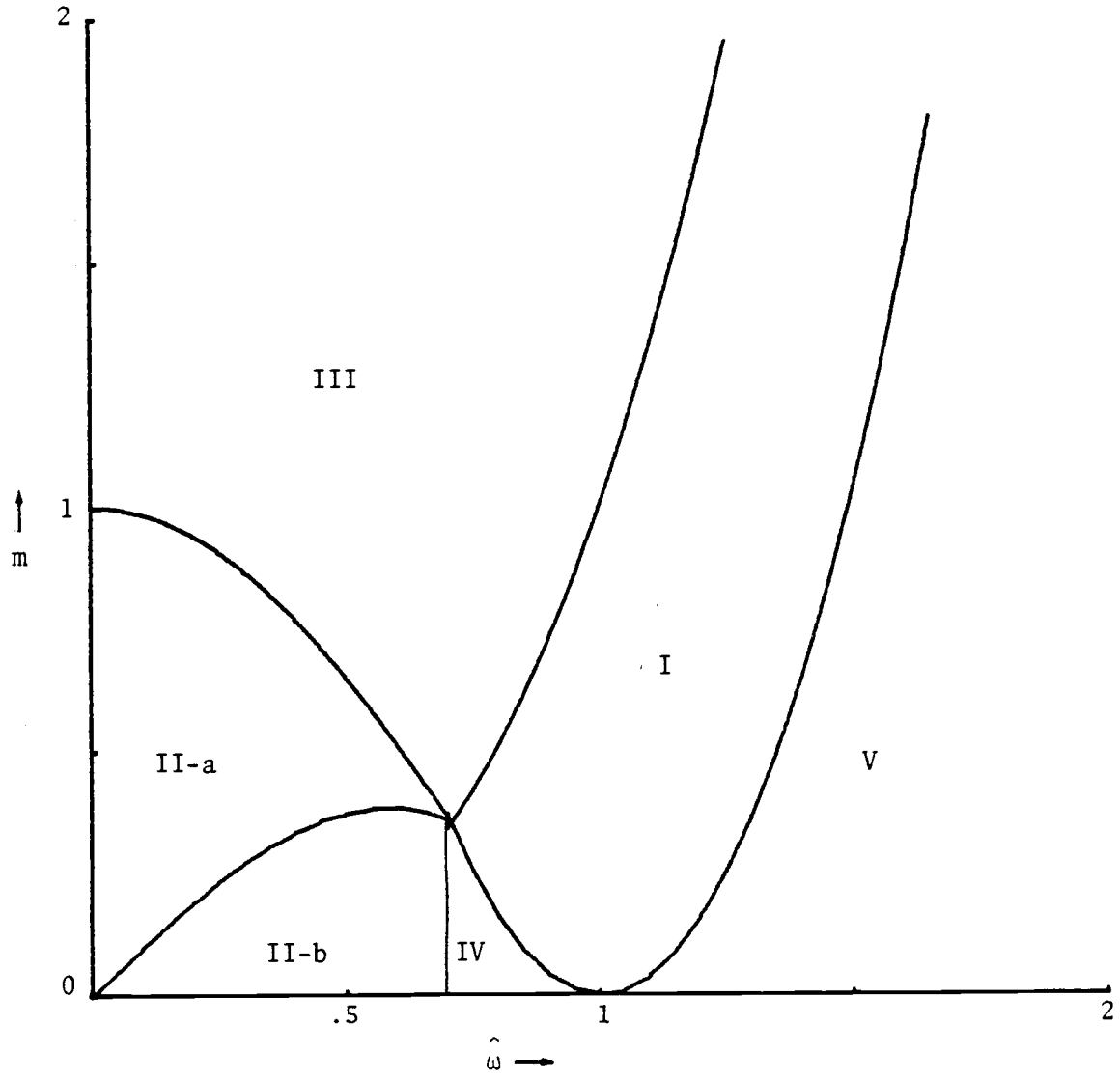

Fig. III-1. Oscillating boundary layers in parameter space $(m,\hat{\omega})$ Subdivisions are facilitated by two-term balances in Eq. (III-4).

TABLE I. OSCILLATING STRATIFIED BOUNDARY LAYERS

Name	Dimensionless Thickness	Restriction & Regions	Relative order of magnitude	Scaled governing equations	Remarks
Stokes	$\left(\frac{E}{\hat{\omega}}\right)^{1/2}$	$\hat{\omega} \gg \frac{1}{\sqrt{2}}$, $m \ll \hat{\omega}^3$ I, IV, V	u v w θ p $\frac{\hat{\omega}(\hat{\omega}E)^{1/2}}{m}$, $\frac{(\hat{\omega}E)^{1/2}}{m}$, $\frac{\hat{\omega}}{B^2}$, 1, $\left(\frac{E}{\hat{\omega}}\right)^{1/2}$	$-i\hat{\omega}u - \frac{v}{\hat{\omega}^2} = \frac{d^2u}{d\eta^2}$, $-i\theta + w = \frac{d^2\theta}{d\eta^2}$ $-iv + u = \frac{d^2v}{d\eta^2}$, $u + \frac{dw}{d\eta} = 0$ $\frac{dp}{d\eta} = \theta$	Acceleration, frictional force & weak Coriolis force in balance
Oscillating Ekman ($E^{1/2}$-layer)	$\left(\frac{E}{\sqrt{1-\hat{\omega}^2}}\right)^{1/2}$	$\hat{\omega} \ll \frac{1}{\sqrt{2}}$, $m \ll (1-\hat{\omega}^2)^{3/4}$ II-a, II-b	$\frac{E^{1/4}(1-\hat{\omega}^2)^{3/4}}{m}$, $\frac{E^{1/4}(1-\hat{\omega}^2)^{1/4}}{m}$, $\frac{(1-\hat{\omega}^2)^{1/2}}{B^2}$, 1, $\left(\frac{E}{\sqrt{1-\hat{\omega}^2}}\right)^{1/2}$	$-i\frac{\hat{\omega}}{\sqrt{1-\hat{\omega}^2}}u - \frac{v}{1-\hat{\omega}^2} = \frac{d^2u}{d\eta^2}$, $w = \frac{d^2\theta}{d\eta^2}$ $u = \frac{d^2v}{d\eta^2}$, $u + \frac{dw}{d\eta} = 0$ $\frac{dp}{d\eta} = \theta$	Coriolis force, frictional force & weak acceleration in balance
$E^{1/3}$-layer	$\left(\frac{E}{B}\right)^{1/3}$	$m \gg \hat{\omega}^3$, $m \gg (1-\hat{\omega}^2)^{3/4}$ III	$\frac{1}{B}$, $\frac{1}{Bm^{1/3}}$, $\frac{m^{1/3}}{B^2}$, 1, $\left(\frac{E}{B}\right)^{1/3}$	$-v = m^{2/3}(P + \frac{d^2u}{d\eta^2})$, $w = \frac{d^2\theta}{d\eta^2}$ $u = \frac{d^2v}{d\eta^2}$, $u + \frac{dw}{d\eta} = 0$ $\frac{dp}{d\eta} = \theta$	Hydrostatically-perturbed pressure gradient force, frictional force & weak Coriolis force in balance.
Stokes-Ekman ($E^{1/2}$-layer)	$\left(\frac{E\hat{\omega}}{1-\hat{\omega}^2}\right)^{1/2}$	$\hat{\omega} \gg \frac{1}{\sqrt{2}}$, $m \ll \frac{(1-\hat{\omega}^2)^2}{\hat{\omega}}$ IV	$\frac{[E\hat{\omega}(1-\hat{\omega}^2)]^{1/2}}{m}$, $\frac{\hat{\omega}}{B^2}$, $\left(\frac{E\hat{\omega}}{1-\hat{\omega}^2}\right)^{1/4}$ $\frac{[E(1-\hat{\omega}^2)]^{1/2}}{m\sqrt{\hat{\omega}}}$, 1,	$-i\hat{\omega}^2u - v = (1-\hat{\omega}^2)\frac{d^2u}{d\eta^2}$, $-i\theta + w = 0$ $-iv + u = 0$, $u + \frac{dw}{d\eta} = 0$ $\frac{dp}{d\eta} = \theta$	Acceleration, frictional force and weak Coriolis force in balance
Stokes-$E^{1/3}$ ($E^{1/4}$-layer)	$\left(\frac{E\hat{\omega}}{B^2}\right)^{1/4}$	$m \ll \hat{\omega}^3$, $m \gg \frac{(1-\hat{\omega}^2)^2}{\hat{\omega}}$ I	$\frac{1}{B}\left(\frac{\hat{\omega}^3}{m}\right)^{1/4}$, $\frac{\hat{\omega}}{B^2}$, $\frac{(m\hat{\omega})^{1/4}}{B}$ $\frac{1}{B(m\hat{\omega})^{1/4}}$, 1,	$P + \frac{d^2u}{d\eta^2} = 0$, $-i\theta + w = 0$ $u = iv$, $u + \frac{dw}{d\eta} = 0$ $\frac{dp}{d\eta} = \theta$	Hydrostatically-perturbed pressure gradient force & frictional force in balance
Oscillating Lineykin	$\left(\frac{1-\hat{\omega}^2}{B^2}\right)^{1/2}$	$m \ll (1-\hat{\omega}^2)^{3/2}$, $m \ll \frac{(1-\hat{\omega}^2)^2}{\hat{\omega}}$ $m < \hat{\omega}(1-\hat{\omega}^2)$ II-b, IV	$\frac{\hat{\omega}}{B(1-\hat{\omega}^2)^{1/2}}$, $\frac{\hat{\omega}}{B^2}$, $\left(\frac{1-\hat{\omega}^2}{B^2}\right)^{1/2}$ $\frac{1}{B(1-\hat{\omega}^2)^{1/2}}$, 1,	$-i\hat{\omega}^2u - v = (1-\hat{\omega}^2)P$, $-i\theta + w = 0$ $-iv + u = 0$, $u + \frac{dw}{d\eta} = 0$ $\frac{dp}{d\eta} = \theta$	Hydrostatically-perturbed pressure gradient force, acceleration and Coriolis in balance
		$m \ll (1-\hat{\omega}^2)^{3/4}$, $m \ll \frac{(1-\hat{\omega}^2)^2}{\hat{\omega}}$ $m > \hat{\omega}(1-\hat{\omega}^2)$ II-a	$\frac{m}{B(1-\hat{\omega}^2)^{1/2}}$, $\frac{E}{1-\hat{\omega}^2}$, $\left(\frac{1-\hat{\omega}^2}{B^2}\right)^{1/2}$ $\frac{1}{B(1-\hat{\omega}^2)^{1/2}}$, 1,	$-v = (1-\hat{\omega}^2)P$, $w = \frac{d^2\theta}{d\eta^2}$ $u = \frac{d^2v}{d\eta^2}$, $u + \frac{dw}{d\eta} = 0$ $\frac{dp}{d\eta} = \theta$	Coriolis force & hydrostatically-perturbed pressure gradient force in balance

boundary layers. In fact all terms in Eq. (III-4) may sometimes be simultaneously important. In the next section, however, we consider special cases which appear to be of particular interest for mid-latitude flow situations. Particular emphasis is placed on the vertical structure of the cross-isobar flow and vertical motion, and the dependence of such a structure on $\hat{\omega}$ and m for synoptic and diurnal-scale motions forced by surface temperature perturbations.

C. Boundary Layers Driven by the Surface Temperature Forcing

For the case where the flow is driven by boundary temperature perturbations with dimensional amplitude $\Delta\theta$, the following boundary conditions are applied to the system Eq. (III-3):

$$\begin{aligned} &u',v',w' = 0, \quad \theta' = \Delta\hat{\theta} \qquad \text{at } \eta = 0 \\ &u',v',w',\theta' \to 0 \quad \text{as } \eta \to \text{large} \end{aligned} \tag{III-5}$$

where $\Delta\hat{\theta} = \frac{gH}{fLV}\frac{\Delta\theta}{\theta_o}$ is the scaled amplitude of the potential temperature perturbation. If the motion is driven by time-dependent surface temperature perturbations, the characteristic velocity amplitude V is assumed to be $O\left(\frac{gH}{fL}\frac{\Delta\theta}{\theta_o}\right)$ so that $\Delta\hat{\theta}$ is O(1). That is, the amplitude of the surface temperature perturbation $\Delta\theta$ could be expressed in terms of a geostrophic wind field of amplitude $O\left(\frac{gH}{fL}\frac{\Delta\theta}{\theta_o}\right)$. However, we must assume $\Delta\theta << \Delta\theta_o$ to make the above perturbation assumption applicable, where $\Delta\theta_o$ is the basic state potential temperature thickness. As a numerical example for typical mid-latitude synoptic-scale motions, we choose $g = 10\text{m sec}^{-2}$, $f = 10^{-4}$ sec $^{-1}$, $L = 10^6\text{m}$, $\theta_o = 285^\circ\text{K}$, $H = 5\sim10 \times 10^3\text{m}$, $\frac{d\theta_o}{dz} = 3 \sim 10 \times 10^{-3}\ ^\circ\text{Km}^{-1}$, and $\Delta\theta = 0 \sim 5^\circ\text{K}$ in which

case $\Delta\theta_o$ varies from 30~50°K and V varies from 0~17 m sec^{-1}.

To examine any one of the flow regimes in Fig. III-1 we must restrict the values of parameters B^2, E, and $\hat{\omega}$. However, a proper re-scaling of variables can reduce the problem to a two-parameter system in B^2E and $\hat{\omega}$ as indicated in Table 1. This is obtained by introducing the following scaling;

$$\begin{aligned} \theta' &= \theta \\ \delta &= E^{\frac{1}{2}} \\ w' &= Ew \\ u' &= E^{\frac{1}{2}}u \\ v' &= E^{\frac{1}{2}}v \\ p' &= E^{\frac{1}{2}}p \end{aligned} \qquad \text{(III-6)}$$

Substituting Eq. (III-6) into Eq. (III-3), we find

$$-i\hat{\omega}u - v = p + \frac{d^2u}{d\eta^2} \qquad \text{(III-7-a)}$$

$$-i\hat{\omega}v + u = \frac{d^2v}{d\eta^2} \qquad \text{(III-7-b)}$$

$$\frac{dp}{d\eta} = \theta \qquad \text{(III-7-c)}$$

$$-i\hat{\omega}\theta + mw = \frac{d^2\theta}{d\eta^2} \qquad \text{(III-7-d)}$$

$$u + \frac{dw}{d\eta} = 0 \qquad \text{(III-7-e)}$$

where $m = B^2E$. The boundary conditions are given in Eq. (III-5) if one drops the prime notation.

When $m \ll 1$ and $\hat{\omega} < 1$, we notice from Table 1 and Fig. III-1 that Eq. (III-7) governs the three prototype boundary layers; the Ekman

layer, the oscillating Lineykin layer, and the thermal Stokes layer. The point is that the Ekman layer is associated with the interaction between frictional effects and the Coriolis force, the Lineykin layer is associated with the stratification, and the thermal Stokes layer is associated with the oscillating forcing stimulus.

Eliminating all dependent variables except p in Eq. (III-7), we then obtain

$$\left(\frac{d^2}{d\eta^2} + i\hat{\omega} \right)\left(\frac{d^6}{d\eta^6} + 2\hat{\omega} i \frac{d^4}{d\eta^4} + (1-\hat{\omega}^2) \frac{d^2}{d\eta^2} - m \right) p = 0 \qquad \text{(III-8)}$$

Without loss of the essential physics, we consider the atmosphere to be of infinite depth so that we eliminate the top boundary effects. Then we may assume the solution of Eq. (III-8) to be of the form

$$p = \sum_{i=1}^{4} C_i e^{-\alpha_i \eta}$$

where C_i is constant and α_is are the roots of the following equation

$$(\alpha_i^2 + i\hat{\omega})(\alpha_i^6 + 2\hat{\omega} i \alpha_i^4 + (1-\hat{\omega}^2)\alpha_i^2 - m) = 0 \qquad \text{(III-9)}$$

The roots which correspond to flow regions II-a, II-b and IV in Fig. III-1 are approximately (see Appendix IV)

$$\alpha_S = \left(\frac{\hat{\omega}}{2} \right)^{1/2} (1-i)$$

$$\alpha_L^2 = \frac{m}{1-\hat{\omega}^2} + O(m^2) \qquad \text{(III-10)}$$

$$\alpha_{1,2}^2 = - \frac{m}{2(1-\hat{\omega}^2)} - (\hat{\omega} \pm 1)i + O(m^2)$$

α_S, α_L and $\alpha_{1,2}$ are easily identified as the inverse thicknesses of

the thermal Stokes, oscillating Lineykin, and oscillating stratified Ekman layers. Note that only four boundary conditions are required to solve Eq. (III-8); one for the thermal Stokes layer, one for the oscillating Lineykin layer and two for the oscillating stratified Ekman layer. These boundary conditions are given in Eq. (III-5).

1) Thermal Stokes Layer

In this layer, flows are driven by temperature diffusion while in the conventional Stokes layer which is given in Table 1 the entire flow is generated by momentum diffusion.

The governing equations for the thermal Stokes-layer variables would be equivalent to $\left(\frac{d^2}{d\eta^2} + i\hat{\omega}\right)p_s = 0$ where the subscript s represents the thermal Stokes-layer contribution. We notice that, since $\left(\frac{d^2}{d\eta^2} + i\hat{\omega}\right)p_s = 0$, it follows that $\left(\frac{d^2}{d\eta 2} + i\hat{\omega}\right)\theta_s = 0$ and consequently, from Eq. (III-7) that $w_s = u_s = 0$, Therefore, cross-isobar flow and vertical motion are produced only by the oscillating Lineykin-layer and the Ekman-layer parts of the solutions. The governing equations of the thermal Stokes layer are

$$-v_s = p_s$$

$$\frac{dp_s}{d\eta} = \theta_s \qquad \text{(III-11)}$$

$$\left(\frac{d^2}{d\eta^2} + i\hat{\omega}\right)p_s = 0 \quad \left[\text{or } \left(\frac{d^2}{d\eta^2} + i\hat{\omega}\right)\theta_s = 0\right]$$

The general solutions are

$$P_s = C_s \exp\left[-\sqrt{\frac{\hat{\omega}}{2}}\,(1-i)\eta\right] \qquad \text{(III-12)}$$

$$\theta_S = -\sqrt{\frac{\hat{\omega}}{2}}\,(1-i)C_S \exp\left[-\sqrt{\frac{\hat{\omega}}{2}}\,(1-i)\eta\right] \qquad \text{(III-12)}$$

$$v_S = -C_S \exp\left[-\sqrt{\frac{\hat{\omega}}{2}}\,(1-i)\eta\right]$$

where C_S is a constant which will be determined later by application of the boundary conditions.

2) Oscillating Lineykin Layer

For $\hat{\omega}<1$, the oscillating Lineykin layer represents regions II and IV in Fig. III-1; however, further subdivisions are possible according to the basic governing dynamics; if the diffusive processes play a dominant role compared with the local accelerations, which is equivalent to the restriction of $m>\hat{\omega}(1-\hat{\omega}^2)$ (region II-a in Fig. III-1), the conventional Lineykin layer is recovered. The governing equations for this layer are:

$$-v_L = P_L$$

$$u_L = \frac{d^2 v_L}{d\eta^2}$$

$$\frac{dp_L}{d\eta} = \theta_L \qquad \text{(III-13)}$$

$$mw_L = \frac{d^2\theta_L}{d\eta^2}$$

$$u_L + \frac{dw_L}{d\eta} = 0$$

where the subscript L indicates the oscillating Lineykin layer contribution. On the other hand, if the local accelerations play a dominant

role compared with the frictional effect $m<\hat{\omega}(1-\hat{\omega}^2)$, the oscillating Lineykin layer occurs. The governing equations for this layer are

$$
\begin{aligned}
&-i\hat{\omega}u_L - v_L = p_L \\
&-i\hat{\omega}v_L + u_L = 0 \\
&\frac{dp_L}{d\eta} = \theta_L \\
&-i\hat{\omega}\theta_L + mw_L = 0 \\
&u_L + \frac{dw_L}{d\eta} = 0
\end{aligned}
\qquad \text{(III-14)}
$$

Regions II-b and IV in Fig. III-1 represent the oscillating Lineykin layers. To distinguish between these possible two types of Lineykin layers, we will hereafter refer to the former as the "Lineykin layer", and the latter the "oscillatory Lineykin layer."

We notice that for a given value of m, the oscillatory Lineykin layer is bounded in an intermediate frequency range, with the Lineykin layer at lower frequencies and the $E^{\frac{1}{4}}$-layer at higher frequencies (Fig. III-1).

From Eq. (III-13) we obtain the general solutions for the Lineykin layer which are

$$
\begin{aligned}
p_L &= C_L \exp\left[-\sqrt{m}\eta\right] \\
\theta_L &= -\sqrt{m}\, C_L \exp\left[-\sqrt{m}\eta\right] \\
w_L &= -\sqrt{m}\, C_L \exp\left[-\sqrt{m}\eta\right] \\
v_L &= -C_L \exp\left[-\sqrt{m}\eta\right] \\
u_L &= -mC_L \exp\left[-\sqrt{m}\eta\right]
\end{aligned}
\qquad \text{(III-15)}
$$

Here we have neglected the terms of order higher than $O(\hat{\omega}^2)$ in view of the restriction $\hat{\omega}(1-\hat{\omega}^2)<m<<1$.

For the oscillatory Lineykin layer, we have

$$
\begin{aligned}
p_L &= C_L \exp\left[-\left(\frac{m}{1-\hat{\omega}^2}\right)^{\frac{1}{2}} \eta\right] \\
\theta_L &= -\left(\frac{m}{1-\hat{\omega}^2}\right)^{\frac{1}{2}} C_L \exp\left[-\left(\frac{m}{1-\hat{\omega}^2}\right)^{\frac{1}{2}} \eta\right] \\
v_L &= -\frac{C_L}{1-\hat{\omega}^2} \exp\left[-\left(\frac{m}{1-\hat{\omega}^2}\right)^{\frac{1}{2}} \eta\right] \\
w_L &= -i\left(\frac{\hat{\omega}^2}{m(1-\hat{\omega}^2)}\right)^{\frac{1}{2}} C_L \exp\left[-\left(\frac{m}{1-\hat{\omega}^2}\right)^{\frac{1}{2}} \eta\right] \\
u_L &= -\frac{i\hat{\omega}}{1-\hat{\omega}^2} C_L \exp\left[-\left(\frac{m}{1-\hat{\omega}^2}\right)^{\frac{1}{2}} \eta\right]
\end{aligned}
\qquad \text{(III-16)}
$$

where C_L is a constant which will be determined later on in application of proper boundary conditions. We notice that Eq. (III-16) reduces to Eq. (III-15) when $\hat{\omega} = m<<1$.

3) Ekman Layer

Since the governing equations for the accelerated stratified Ekman layer are the same as given in Eq. (III-7), the general solutions for this layer are

$$
\begin{aligned}
P_\varepsilon &= \sum_{j=1}^{2} C_j e^{-\mu_j \eta} \\
\theta_\varepsilon &= -\sum_{j=1}^{2} C_j \mu_j e^{-\mu_j \eta} \\
w_\varepsilon &= -\frac{1}{m}\left[\sum_{j=1}^{2} (\mu_j^2 + i\hat{\omega})\, \mu_j c_j e^{-\mu_j \eta}\right]
\end{aligned}
\qquad \text{(III-17)}
$$

$$u_\varepsilon = -\frac{1}{m}\left[\sum_{j=1}^{2}(\mu_j^2 + i\hat{\omega})\mu_j^2 c_j e^{-\mu_j \eta}\right]$$

$$v_\varepsilon = \frac{1}{m}\left[\sum_{j=1}^{2}\left\{(\mu_j^2 + i\hat{\omega})^2\,\mu_j^2 - m\right\} c_j e^{-\mu_j \eta}\right]$$

where the subscript ε indicates the Ekman layer contribution, and

$$\mu_1 \cong \left[\tfrac{1}{2}\left(1-\hat{\omega}-\frac{m}{2(1-\hat{\omega}^2)}\right)\right]^{\frac{1}{2}} + i\left[\tfrac{1}{2}\left(1-\hat{\omega}+\frac{m}{2(1-\hat{\omega}^2)}\right)\right]^{\frac{1}{2}}$$

$$\mu_2 \cong \left[\tfrac{1}{2}\left(1+\hat{\omega}-\frac{m}{2(1-\hat{\omega}^2)}\right)\right]^{\frac{1}{2}} - i\left[\tfrac{1}{2}\left(1+\hat{\omega}+\frac{m}{2(1-\hat{\omega}^2)}\right)\right]^{\frac{1}{2}} \qquad \text{(III-18)}$$

Note that the vertical structure of the accelerated stratified Ekman layer is

$$\exp\left[-\mu_j \eta\right] = \exp\left[-E^{-\frac{1}{2}}\mu_j z\right] = \exp\left[-\frac{1}{\sqrt{2E}}\left\{\left(1 \mp \hat{\omega} - \frac{m}{2(1-\hat{\omega}^2)}\right)^{\frac{1}{2}} \mp i\left(1 \mp \hat{\omega} + \frac{m}{2(1-\hat{\omega}^2)}\right)^{\frac{1}{2}}\right\} z\right] \qquad \text{(III-18)}$$

If we denote the e-folding thickness of boundary layer by δ^* and a measure of the wavelength of the vertical oscillations of the velocity profiles by ℓ^*, then

$$\delta^* = \frac{\sqrt{2E}}{\left[1 \mp \hat{\omega} - \frac{m}{2(1-\hat{\omega}^2)}\right]^{\frac{1}{2}}} \qquad \text{(III-19-a)}$$

$$\ell^* = \frac{\sqrt{2E}}{\left[1 \mp \hat{\omega} + \frac{m}{2(1-\hat{\omega}^2)}\right]^{\frac{1}{2}}} \qquad \text{(III-19-b)}$$

The numerator of Eq. (III-19) represents the thickness of the classical Ekman layer and the denominator indicates the modifications due to accelerations and the stratification. The second and third terms in the denominator are, respectively, the influence of the thermal Stokes

layer and oscillatory Lineykin layer on the Ekman layer since $\hat{\omega} = \frac{\delta_\varepsilon}{\delta_S}^2$ and $\frac{m}{2(1-\hat{\omega}^2)} = \left(\frac{\delta_\varepsilon}{\delta_L}\right)^2$, where δ_ε, δ_S and δ_L are, respectively, the thickness of classical Ekman layer, thermal Stokes layer and oscillatory Lineykin layer. Since the vertical motion affects the thickness and the vertical wavelength of the Ekman layer, and since the flow of the thermal Stokes layer is nondivergent, the net influence of the thermal Stokes layer on δ^* and ℓ^* is zero. However, the influence of stratification on these parameters is of significance. Note that the e-folding thickness of the Ekman layer increases with stratification. This behavior is due to the increase of low-level shear induced by the Lineykin layer. In geophysical flows where the exchange coefficient decreases with elevation, this interaction is likely to be of less importance. The vertical wavelength of the oscillatory, horizontal velocities decreases with increasing stratification. This implies that the velocity components (and divergence) change their signs with elevation within the e-folding boundary layer thickness. Therefore, the resulting boundary layer pumping at a given elevation greatly diminishes with increasing stratification. In other words, as the stratification increases, the thickness of the Lineykin layer (or oscillatory Lineykin layer) becomes thinner. Mass continuity requires that the convergence in the Ekman layer must be compensated by the divergence in the Lineykin layer. Consequently, the divergence within the Lineykin layer is intensified near the bottom with increasing stratification so that the net boundary-layer pumping is considerably mitigated.

D. Approximate Solutions

Direct application of boundary conditions Eq. (III-5) to the solutions Eqs. (III-12), (III-15) (or (III-16)) and (III-17) can determine the constants C_S, C_L, C_1 and C_2 as in Kuo (1973) and Leetmaa (1971). Although solution is possible without further approximation, at least for some regions of the m-$\hat{\omega}$ parameter space, it is physically more illuminating to employ the type of perturbation analysis used in Leetmaa (1971) and Allen (1972). Here the solution is considered to consist of three contributions; the thermal Stokes layer, the Lineykin layer (or oscillatory Lineykin layer) and the Ekman layer.

i) Case 1; $\hat{\omega}(1-\hat{\omega}^2) < m \ll 1$

Region (II-a) in Fig. III-1 belongs to this case. The scaling of the lowest order terms with respect to imposed surface temperature perturbation in the governing equations for the thermal Stokes layer (III-12), Lineykin layer (III-15) and Ekman layer (III-17) is

$$\theta_S = O\left(\sqrt{\frac{\hat{\omega}}{m}}\right), \quad \theta_L = O(1), \quad \theta_\varepsilon = O(m)$$

$$v_S = O\left(\frac{1}{\sqrt{m}}\right), \quad v_L = O\left(\frac{1}{\sqrt{m}}\right), \quad v_\varepsilon = O(1) \qquad \text{(III-20)}$$

$$u_L = O(\sqrt{m}), \quad u_\varepsilon = O(1)$$

$$w_L = O(1), \quad w_\varepsilon = O(1)$$

Because the order of magnitude of the temperature perturbation in the Lineykin-layer solution is larger than it is in the thermal Stokes-layer or in the Ekman-layer solutions, the Lineykin-layer solutions

approximately satisfy the temperature boundary conditions imposed at the surface. Due to the pressure gradient force in the Lineykin layer induced by the surface temperature forcing, Ekman pumping of $0(E\Delta\hat{\theta})$ is induced.

The order that would be followed in the application of the boundary conditions at $\eta=0$ is

$$\begin{aligned} \theta_L &= \Delta\hat{\theta} \\ v_L + v_S &= 0 \\ w_L + w_\varepsilon &= 0 \\ u_L + u_\varepsilon &= 0 \end{aligned} \qquad \text{(III-21)}$$

The first condition in Eq. (III-21) resolves the Lineykin-layer solutions, the second one determines the thermal Stokes-layer solutions and the third and fourth ones give the complete solutions of the Ekman layer. At this moment, it is useful to comment briefly on the physical implication of the second condition in Eq. (III-21). The no-slip boundary condition is initially imposed with regard to the importance of friction adjacent to the boundary. However, the induced wind of the Ekman layer is much smaller than that of the thermal Stokes layer or the Lineykin layer. Therefore, to lowest order, the thermal Stokes and Lineykin flow components in the geostrophic wind direction are of comparable magnitude and of opposite sign at $\eta=0$.

Substituting Eq. (III-21) into Eqs. (III-15), (III-12) and (III-17), we find

$$C_L = -\frac{\Delta\hat{\theta}}{\sqrt{m}} \qquad \text{(III-22)}$$

$$C_s = \frac{\hat{\Delta\theta}}{\sqrt{m}}$$

$$C_1 = \frac{m\hat{\Delta\theta}(\mu_2 - \sqrt{m})}{\mu_1(\mu_2-\mu_1)(\mu_1^2 + i\hat{\omega})} \qquad \text{(III-22 cont'd)}$$

$$C_2 = \frac{m\hat{\Delta\theta}(\mu_1 - \sqrt{m})}{\mu_2(\mu_1-\mu_2)(\mu_2^2 + i\hat{\omega})}$$

where μ_1 and μ_2 are given in Eq. (III-18) and terms of $O(\hat{\omega}^2)$ have been dropped. The approximate solutions are the sum of the solutions given in Eqs. (III-15), (III-12) and (III-17) with constants in Eq. (III-22). The leading order solutions are

$$P = \frac{\hat{\Delta\theta}}{\sqrt{m}}\left[e^{-\sqrt{\frac{\hat{\omega}}{2}}(1-i)\eta} - e^{-\sqrt{m}\eta} + O(m\sqrt{m})\right] \qquad \text{(III-23-a)}$$

$$v = \frac{\hat{\Delta\theta}}{\sqrt{m}}\left[e^{-\sqrt{m}\eta} - e^{-\sqrt{\frac{\hat{\omega}}{2}}(1-i)\eta} + O(\sqrt{m})\right] \qquad \text{(III-23-b)}$$

$$\theta = \hat{\Delta\theta}\left[e^{-\sqrt{m}\eta} + O\left(\sqrt{\frac{\hat{\omega}}{2m}}\right)\right] \qquad \text{(III-23-c)}$$

$$u = \hat{\Delta\theta}\left[\sqrt{m}\, e^{-\sqrt{m}\eta} - \frac{1}{\mu_2-\mu_1}\left\{\mu_1(\mu_2-\sqrt{m})e^{-\mu_1\eta} - \mu_2(\mu_1-\sqrt{m})e^{-\mu_2\eta}\right\}\right] \qquad \text{(III-23-d)}$$

$$w = \hat{\Delta\theta}\left[e^{-\sqrt{m}\eta} - \frac{1}{\mu_2-\mu_1}\left\{(\mu_2-\sqrt{m})e^{-\mu_1\eta} - (\mu_1-\sqrt{m})e^{-\mu_2\eta}\right\}\right] \qquad \text{(III-23-e)}$$

Note that Eqs. (III-23-a) and (III-23-b) do not reduce to the homogeneous limit unless some provision is made to let the applied temperature perturbation at the surface approach zero as the stratification decreases. Such a result was also obtained by Leetmaa (1971) and Stommel and Veronis (1957). We also note that the induced pressure

perturbation and the v-component wind velocity in the thermal Stokes layer become finite as $\hat{\omega} \to 0$, since they are proportional to the vertical integration of the temperature perturbation which is independent of $\hat{\omega}$. The cross-isobar flow (III-23-d) and the vertical motion (III-23-e) can be decomposed into the real part, which is in the phase with the horizontal temperature gradient imposed at the surface, and the imaginary part, which is out of phase with the changing surface temperature.

The profiles of the flow (Eqs. III-23-d) and (III-23-e)) are presented for several different values of the parameter m in Figs. III-2 and III-3. As the stratification increases, the height where the cross-isobar flow u vanished for the first time (i.e. half of the vertical wavelength) shifts downward and is accompanied by a significant reduction of amplitude (Fig. III-2). The reduction of cross-isobar flow and reduction of vertical motion (Fig. III-3) at a given level with increasing stratification can also be explained in terms of pressure adjustments (Lineykin layer) which lead to reduce horizontal pressure gradients at low levels.

When the value of m is larger than 5×10^{-2}, the vertical velocity (Fig. III-3) is reduced by more than 50% of the homogeneous Ekman flow values.

a) Geophysical application

A possible application of the slowly-oscillating case to problems of considerable comtemporary interest is that of the flow driven by the steady or slowly varying surface temperature anomalies (e.g. Spar, 1973; Houghton et al., 1974; Namias, 1976; Chervin and

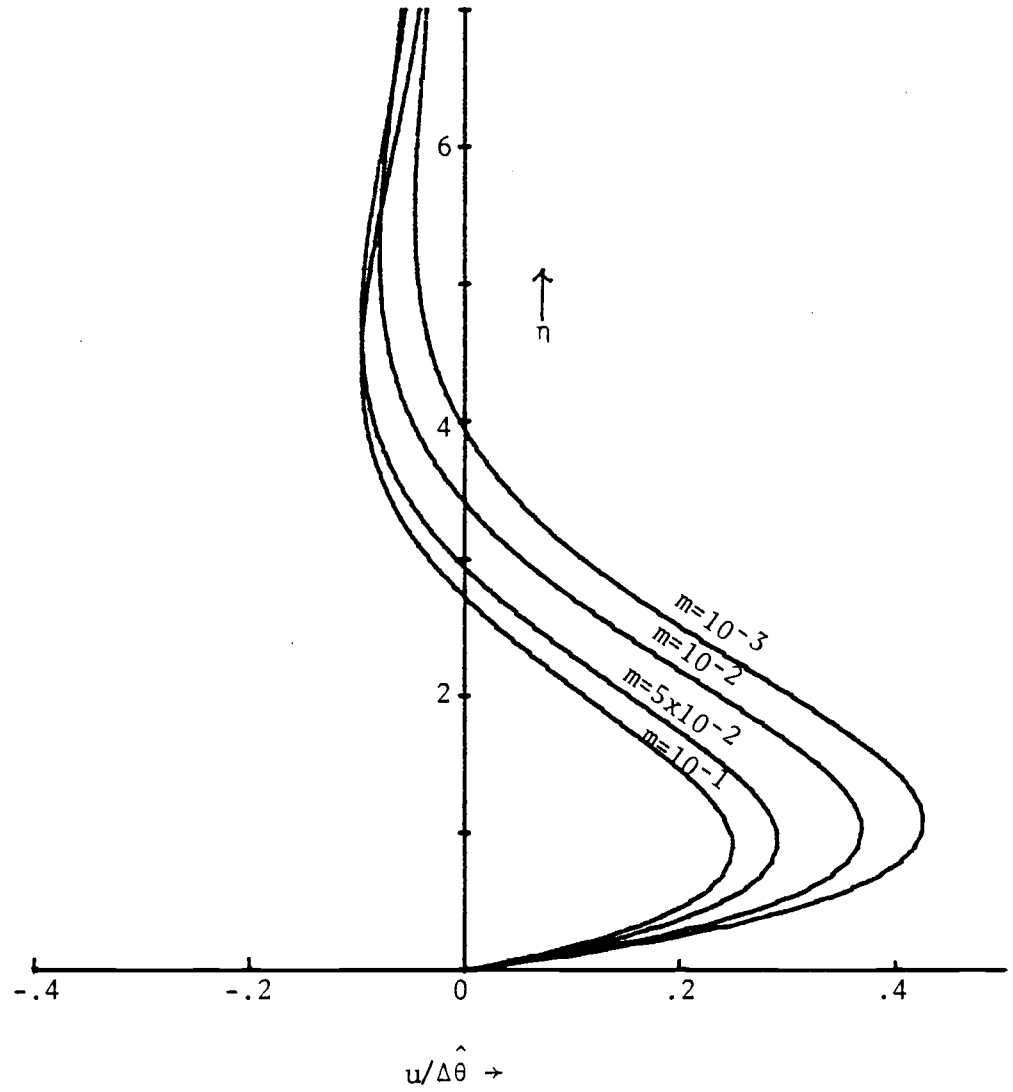

Fig. III-2. Scaled amplitude of the cross-isobar flow Eq. (III-23-d) as a function of height for several different values of m.

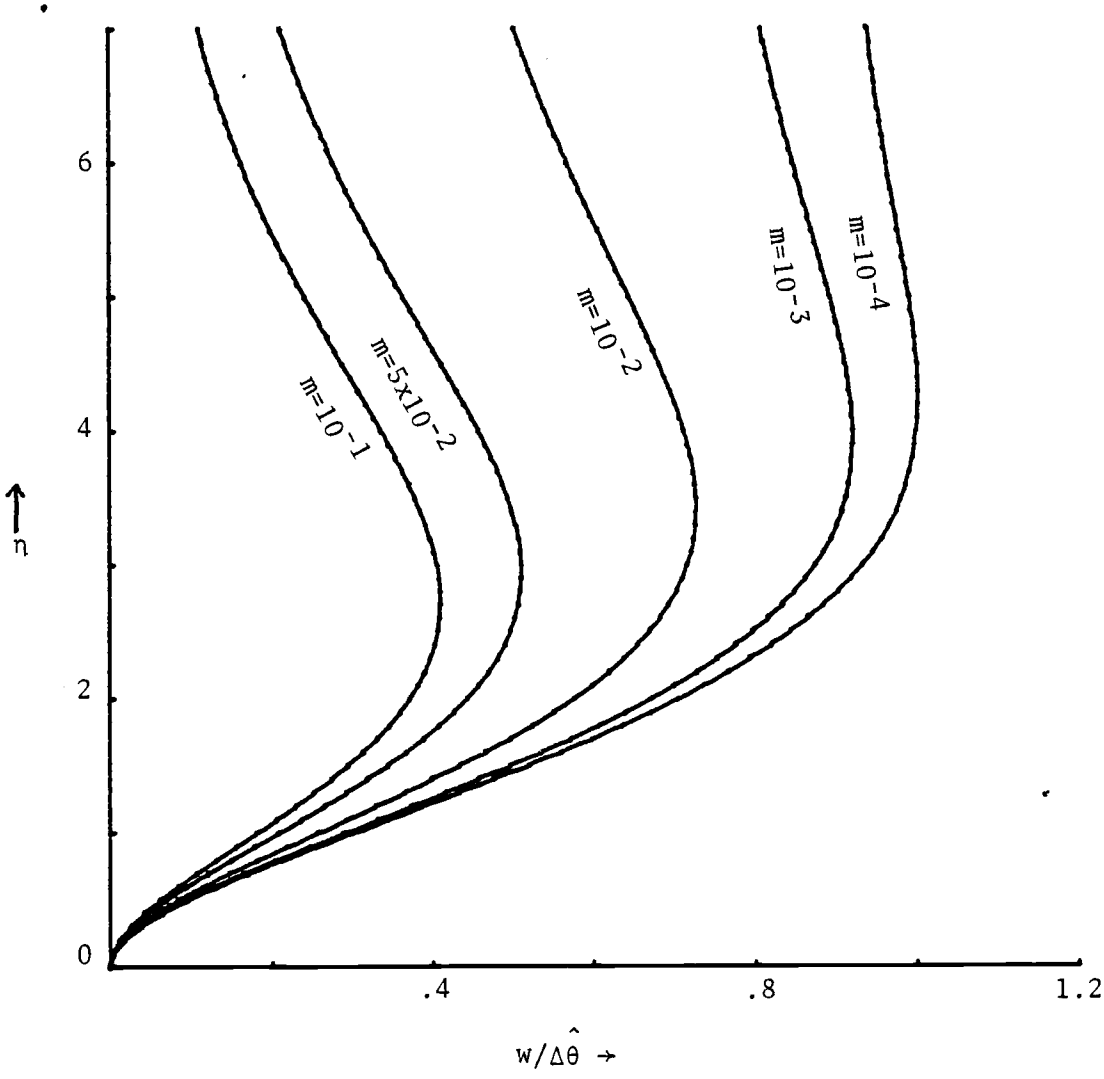

Fig. III-3. Scaled amplitude of the vertical velocity Eq. (III-23-d) as a function of height for several different values of m.

Schneider, 1976). Of particular interest here is the limit $\hat{\omega}\to 0$. The ocean surface temperature anomalies are normally defined as the deviation from the long-term mean, although, here we are interested in such anomalies only with respect to any resulting horizontal gradients of surface temperature. These anomalies may be important for the general circulation of the atmosphere. For example, over the North Pacific, Namias (1976) attempted to show that warm summer sea surface temperature anomalies lead to strong Aleutian lows in fall, resulting in a high-index pattern with a ridge in the West and a trough in the East. This pattern is thought to cause diminution of precipitation over much of the West.

To estimate the potential importance of such effects of sea surface temperature anomalies we let the dimensional amplitude of surface temperature anomaly be $\Delta\theta=2\sim3^{o}K$ suggested by Fig. III-4 after Namias (1976) and also suggested by Houghton et al. (1974) over the North Atlantic. Our simple two-dimensional model cannot include all the features that appear in Fig. III-4, however, basic linear components of the governing dynamics may be resolved. The dimensional forms of Eq. (III-23-d) and (III-23-e) for the case $\hat{\omega}\to 0$ are

$$u^{*} = \left(\frac{K}{f}\right)^{\frac{1}{2}} \frac{g\Delta\theta}{fL\theta_{o}}\left[\sqrt{m}\, e^{-\frac{z}{\delta_L}} - e^{-\frac{\alpha_1 z}{\delta_\varepsilon}}\left\{\sqrt{m}\cos\left(\frac{\alpha_2 z}{\delta_\varepsilon}\right) + \frac{1-\sqrt{m}\alpha_1}{\alpha_2}\sin\left(\frac{\alpha_2 z}{\delta_\varepsilon}\right)\right\}\right]$$

$$w^{*} = \frac{gK\Delta\theta}{f^{2}L^{2}\theta_{o}}\left[e^{-\frac{z}{\delta_L}} - e^{-\left(\frac{\alpha_1 z}{\delta_\varepsilon}\right)}\left\{\cos\left(\frac{\alpha_2 z}{\delta_\varepsilon}\right) + \frac{\alpha_1-\sqrt{m}}{\alpha_2}\sin\left(\frac{\alpha_2 z}{\delta_\varepsilon}\right)\right\}\right]$$

where $\alpha_1 = \left[\frac{1}{2}\left(1-\frac{m}{2}\right)\right]^{\frac{1}{2}}$, $\alpha_2 = \left[\frac{1}{2}\left(1+\frac{m}{2}\right)\right]^{\frac{1}{2}}$, $\delta_L = \frac{fL}{N}$ and $\delta_\varepsilon = \left(\frac{2K}{f}\right)^{\frac{1}{2}}$

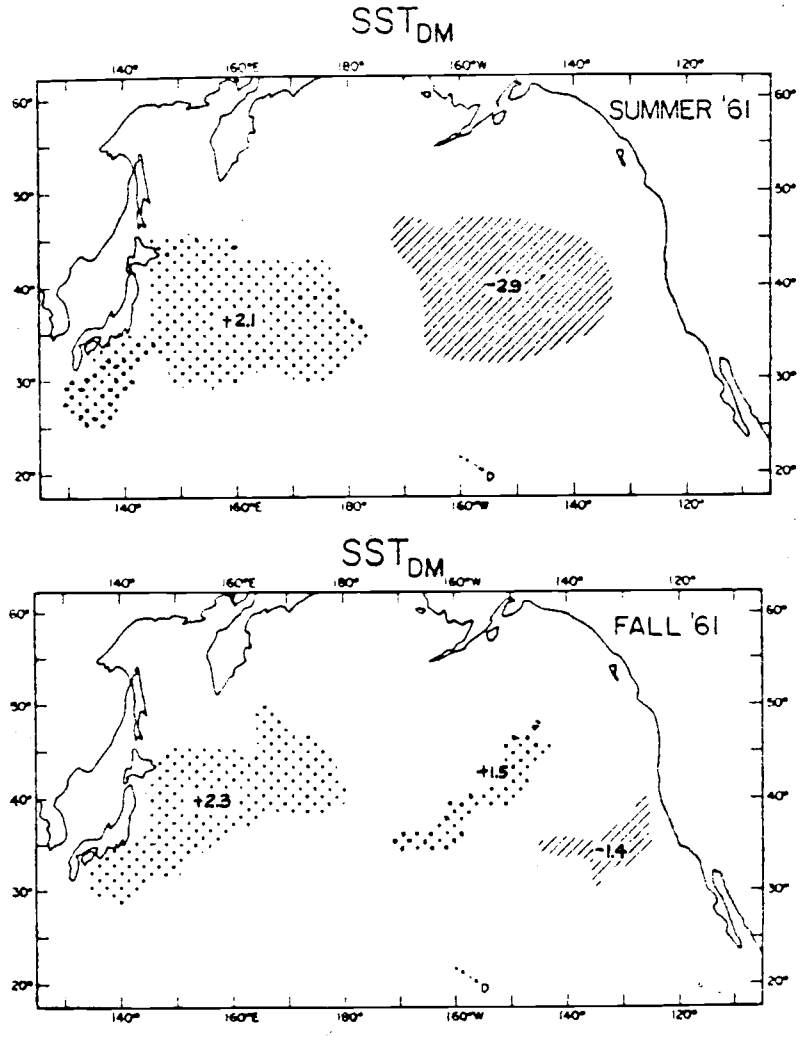

Fig. III-4. Sea surface temperature anomalies for summer (top) and fall (bottom) of 1961 where stippling indicates warm anomalies (>1^{o}F) and shading cold anomalies (After Namias, 1976).

The circulation induced by the surface temperature anomalies is linearly proportional to the amplitude of the anomalies. The dimensional amplitudes of the cross-isobar flow and vertical velocity are, respectively, approximated by $\left(\frac{K}{f}\right)^{\frac{1}{2}} \frac{g\Delta\theta}{fL\theta_o}$ and $\frac{gK\Delta\theta}{f^2L^2\theta_o}$. For the numerical examples of the mid-latitude synoptic-scale surface temperature anomalies, we also assign $L=5\sim10\times10^5$m, $\Delta\theta=2\sim3^oK$, $K=5\sim10 m^2sec^{-1}$, $f=10^{-4}sec^{-1}$, $\theta_o=280^oK$, and we obtain $u^*=2\sim7\times10^{-1}$ m sec^{-1} and $w^*=0.4\sim4\times10^{-4}$ m sec^{-1}. This is considered to be comparable to or less than the boundary layer vertical motions in typical mid-latitude, synoptic-scale systems. However, such vertical motions would likely be of climatic importance. It is, however, worth noting that such an estimate is very sensitive to the choice of horizontal length scale.

ii) Case 2; $\hat{\omega}(1-\hat{\omega}^2)>m>\hat{\omega}^2(1-\hat{\omega}^2)$

This case corresponds to region II-b in Fig. III-1, and can be roughly associated with synoptic-scale flows or perhaps with diurnally-varying flows of small width and substantial stratification. The synoptic-scale case can be associated with interaction between horizontal variations of surface properties, such as heat capacity, and synoptic-scale properties such as cloudiness.

As $\hat{\omega}$ increases, the flow regions II-b and IV in Fig. III-1 are further subdivided into two cases according to the altering governing dynamics; case 2 discussed in this section, where the induced pressure perturbation in the oscillatory Lineykin layer is larger than that in the oscillating Ekman layer for $m>\hat{\omega}^2(1-\hat{\omega}^2)$, and case 3 discussed in the next section, where the thickness of oscillating Ekman layer is no longer thinner than that of oscillatory Lineykin layer for $m<\hat{\omega}^2(1-\hat{\omega}^2)$ so

that the oscillating Ekman layer plays a dominant role on the production of vertical motion.

As long as $\hat{\omega}<1$, the dynamics of the Ekman layer and thermal Stokes layer are not drastically altered by the accelerations. Therefore, we may once again consider the solutions to be made up of three contributions; the thermal Stokes-layer, oscillatory Lineykin-layer and Ekman-layer solutions. Using the order of magnitude analysis for these layers' variables, we find

$$\theta_S = O(1),\ \theta_L = O\left(\left[\frac{m(1-\hat{\omega}^2)}{\hat{\omega}}\right]^{\frac{1}{2}}\right),\quad \theta_\varepsilon = O\left(\left[m\hat{\omega}(1-\hat{\omega}^2)\right]^{\frac{1}{2}}\right)$$

$$v_S = O\left(\frac{1}{\sqrt{\hat{\omega}}}\right),\ v_L = O\left(\frac{1}{\sqrt{\hat{\omega}}}\right),\qquad v_\varepsilon = O\left(\left[\frac{\hat{\omega}(1-\hat{\omega}^2)}{m}\right]^{\frac{1}{2}}\right)$$

$$u_L = O(\sqrt{\hat{\omega}}),\qquad u_\varepsilon = O\left(\left[\frac{\hat{\omega}(1-\hat{\omega}^2)}{m}\right]^{\frac{1}{2}}\right) \qquad \text{(III-24)}$$

$$w_L = O\left(\left[\frac{\hat{\omega}(1-\hat{\omega}^2)}{m}\right]^{\frac{1}{2}}\right),\ w_\varepsilon = O\left(\left[\frac{\hat{\omega}(1-\hat{\omega}^2)}{m}\right]^{\frac{1}{2}}\right)$$

Eq. (III-24) can be also checked from Eqs. (III-12), (III-16), and (III-17). Note that $\frac{1}{\sqrt{\hat{\omega}}} > \left[\frac{\hat{\omega}(1-\hat{\omega}^2)}{m}\right]^{\frac{1}{2}}$. This restriction provides the subdivisions of the flow regimes of II-b and II-c in Fig. III-5. Because the order of magnitude of the temperature perturbation in the thermal Stokes-layer solutions is larger than that in the oscillatory Lineykin-layer or Ekman-layer solutions, the imposed temperature perturbation generates the pressure gradient through temperature diffusive process in the thermal Stokes layer. The generated thermal wind, whose magnitude is $O\left(\frac{1}{\sqrt{\hat{\omega}}}\right)$, is generated by the imposed horizontal temperature gradient and directly affects the oscillatory Lineykin layer. From the second equation of Eq. (III-14) we see that the cross-isobar flow in the

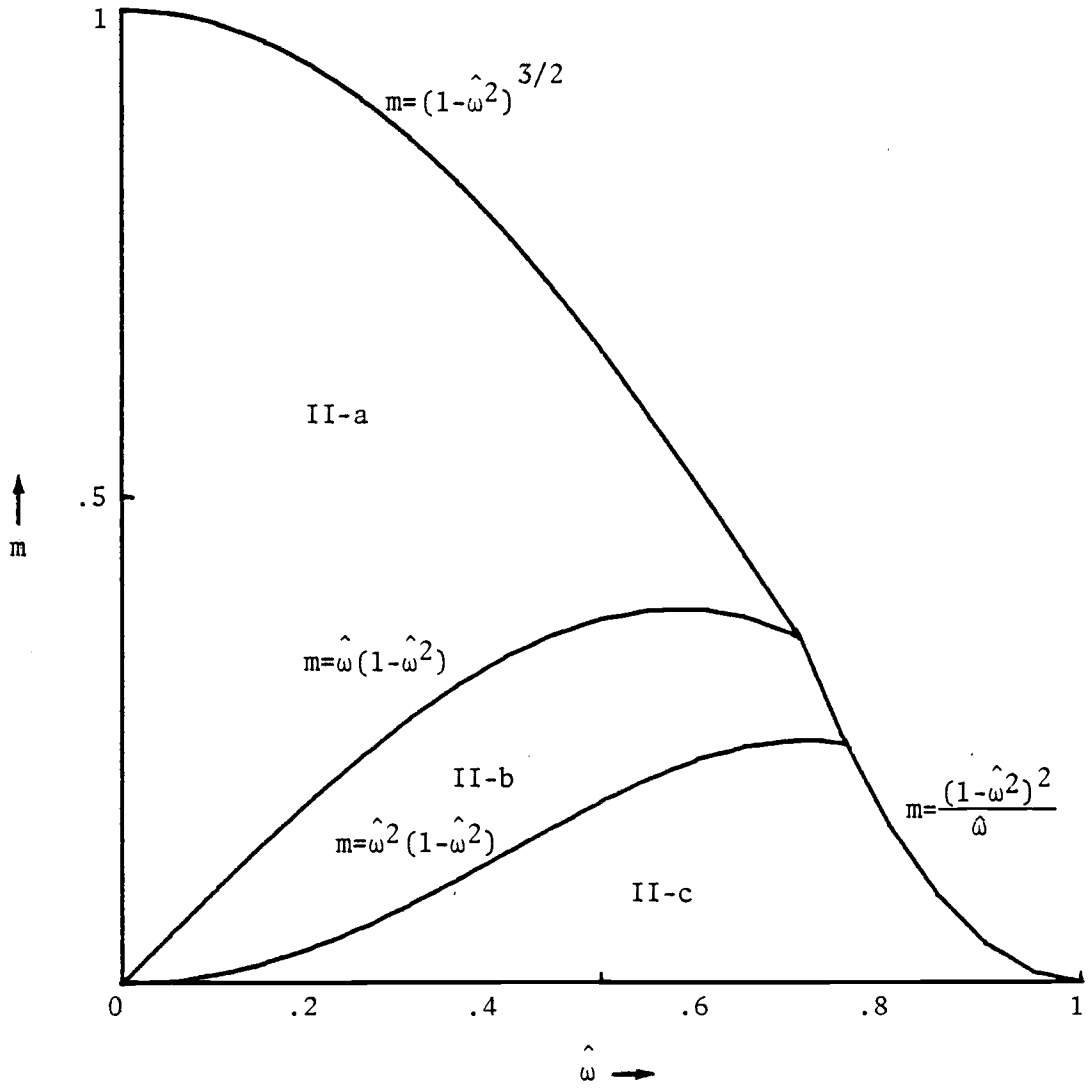

Fig. III-5. Subdivisons of the Oscillating Lineykin layer in parameter space $(m,\hat{\omega})$.

oscillatory Lineykin layer is at most $O(\hat{\omega}v_L)$, while $v_L \sim v_s = O(\frac{1}{\sqrt{\hat{\omega}}})$. Consequently, the isallobaric wind is $O(\sqrt{\hat{\omega}})$, which is proportional to the square root of imposed frequency. We notice that the vertical velocity is at most $O\left(\left[\frac{\hat{\omega}(1-\hat{\omega}^2)}{m}\right]^{\frac{1}{2}}\right)$ which is larger than unity, while the vertical velocity in case 1 is O(1). Therefore, accelerations significantly enhance the vertical motion when the adiabatic cooling term can be balanced by temporal temperature changes instead of temperature diffusion (Kuo, 1973).

The order of application of the boundary conditions at $\eta=0$ is

$$\begin{aligned} \theta_s &= \Delta\hat{\theta} \\ v_s + v_L &= 0 \\ w_L + w_\varepsilon &= 0 \\ u_L + u_\varepsilon &= 0 \end{aligned} \qquad \text{(III-25)}$$

The first condition in Eq. (III-25) determines the thermal Stokes-layer solutions Eq. (III-12), the second condition determines the oscillatory Lineykin-layer solutions Eq. (III-16) and the third and fourth ones provide the necessary conditions to determine the Ekman layer.

The general solution is the sum of these solutions which to lowest order is

$$p = \frac{\Delta\hat{\theta}(1+i)}{\sqrt{2\hat{\omega}}}\left[(1-\hat{\omega}^2)e^{-\sqrt{\frac{m}{1-\hat{\omega}^2}}\eta} - e^{-\sqrt{\frac{\hat{\omega}}{2}}(1-i)\eta} + O(\hat{\omega}\sqrt{m})\right] \qquad \text{(III-26-a)}$$

$$v = \frac{\Delta\hat{\theta}(1+i)}{\sqrt{2\hat{\omega}}}\left[e^{-\sqrt{\frac{\hat{\omega}}{2}}(1-i)\eta} - e^{-\sqrt{\frac{m}{1-\hat{\omega}^2}}\eta} + O\left(\left[\frac{\hat{\omega}^2(1-\hat{\omega}^2)}{m}\right]^{\frac{1}{2}}\right)\right] \qquad \text{(III-26-b)}$$

$$\theta = \Delta\hat{\theta}\left[e^{-\sqrt{\frac{\hat{\omega}}{2}}(1-i)\eta} + O\left(\left[\frac{m(1-\hat{\omega}^2)}{\hat{\omega}}\right]^{\frac{1}{2}}\right)\right] \qquad \text{(III-26-c)}$$

$$u = \sqrt{\frac{\hat{\omega}}{2}}(1-i)\Delta\hat{\theta}\left[e^{-\sqrt{\frac{m}{1-\hat{\omega}^2}}\eta}\sqrt{\frac{1-\hat{\omega}^2}{m}}\cdot\frac{1}{\mu_2-\mu_1}\left\{\left(\mu_1\mu_2\sqrt{\frac{m}{1-\hat{\omega}^2}}-\mu_1\right)\cdot\right.\right.$$

$$\left.\left.e^{-\mu_1\eta} - \left(\mu_1\mu_2-\sqrt{\frac{m}{1-\hat{\omega}^2}}\,\mu_2\right)\cdot e^{-\mu_2\eta}\right\}\right] \qquad \text{(III-26-d)}$$

$$w = \left(\frac{\hat{\omega}(1-\hat{\omega}^2)}{2m}\right)^{\frac{1}{2}}\Delta\hat{\theta}(1-i)\left[e^{-\left(\frac{m}{1-\hat{\omega}^2}\right)^{\frac{1}{2}}\eta} - \frac{1}{\mu_2-\mu_1}\left\{\left(\mu_2-\sqrt{\frac{m}{1-\hat{\omega}^2}}\right)e^{-\mu_1\eta} -\right.\right.$$

$$\left.\left.\left(\mu_1-\sqrt{\frac{m}{1-\hat{\omega}^2}}\right)e^{-\mu_2\eta}\right\}\right] \qquad \text{(III-26-e)}$$

The variations of cross-isobar flow Eq. (III-26-d) and vertical velocity Eq. (III-26-e) with height are respectively plotted in Figs. (III-6-a) and (III-6-b) for $\hat{\omega}=10^{-1}$. Both the amplitudes of cross-isobar flow and vertical velocity decrease with increasing m, as in case 1. However, the amplitudes are more sensitive to stratification when the flow is accelerated as is evident by comparing Figs. III-6-b and III-3.

The influence of accelerations on the cross-isobar flow and the vertical motion is shown in Figs. (III-7-a) and (III-7-b), respectively. As $\hat{\omega}$ increases, both the cross-isobar flow and the vertical velocity are enhanced by accelerations, but the thickness of the boundary layer does not change as mentioned earlier.

iii) Case 3; $m<\hat{\omega}^2(1-\hat{\omega}^2)$

This case corresponds to the flow region II-c in Fig. III-5. For a given value of small m, the oscillatory Lineykin layer only exists within a certain frequency range. The examination of this case allows us to investigate most diurnally-varying motions in the

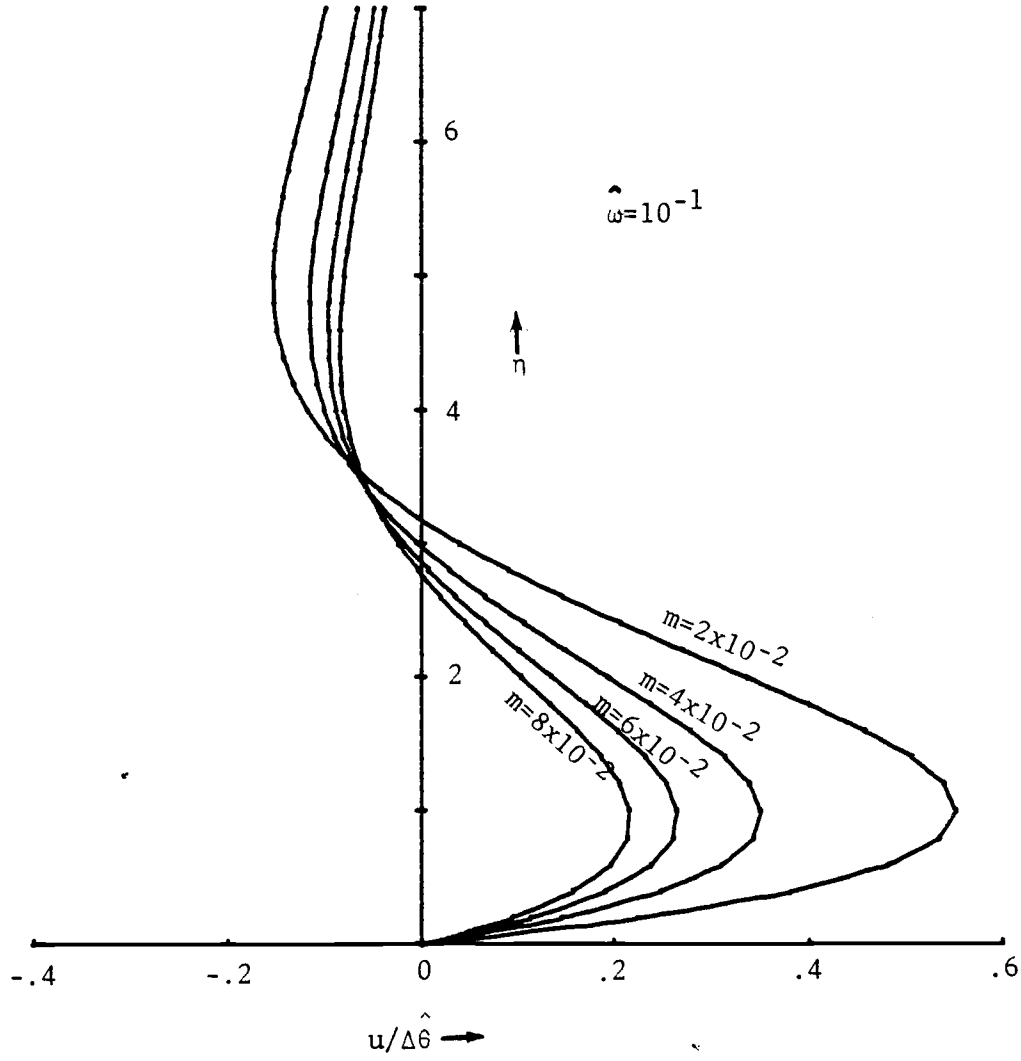

Fig. III-6-a. Scaled amplitude of the cross-isobar flow Eq. (III-25-d) as a function of height for several different values of m and $\hat{\omega}=10^{-1}$.

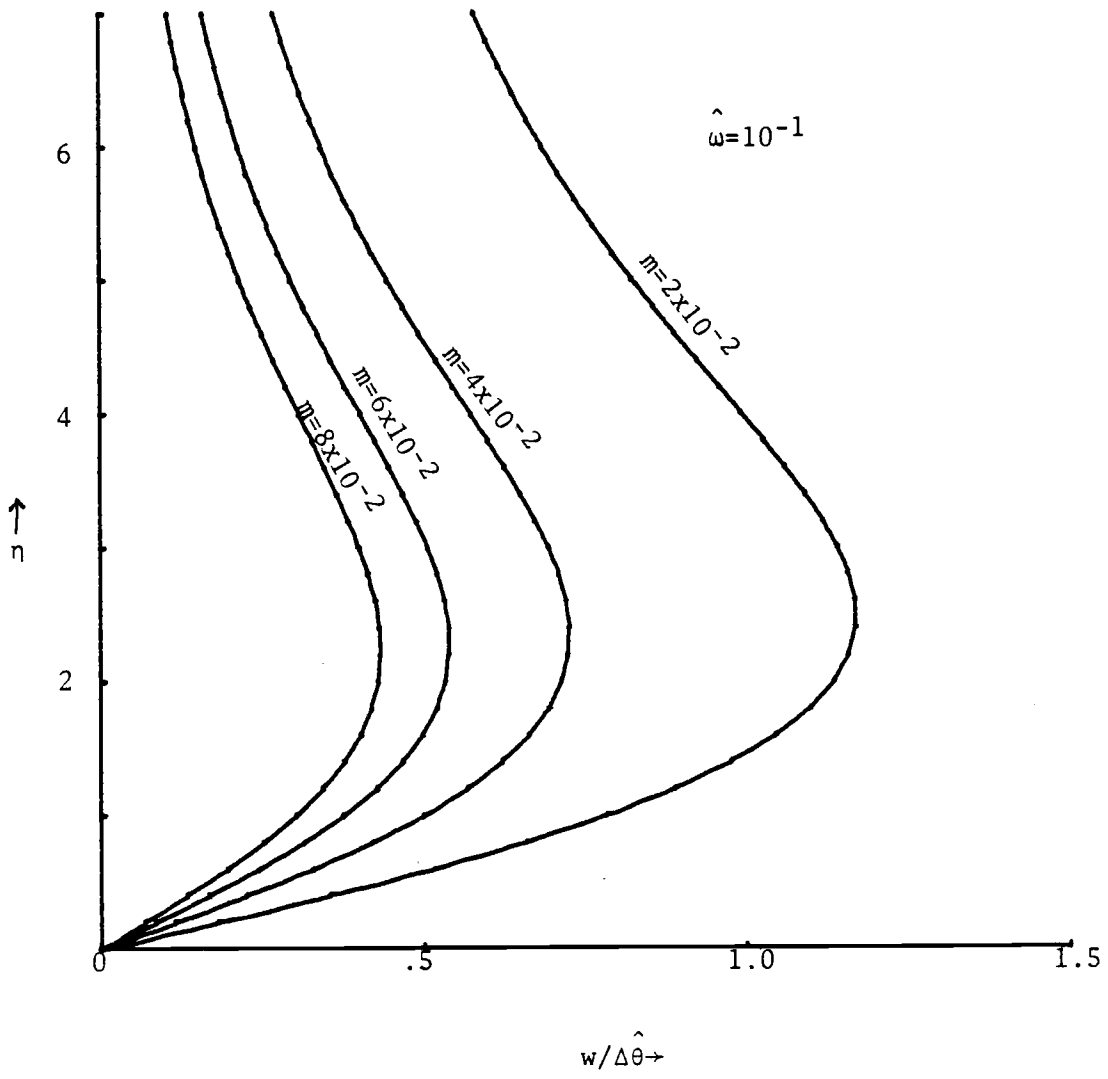

Fig. III-6-b. Scaled amplitude of the vertical velocity Eq. (III-25-e) as a function of height for several different values of m and $\hat{\omega}=10^{-1}$.

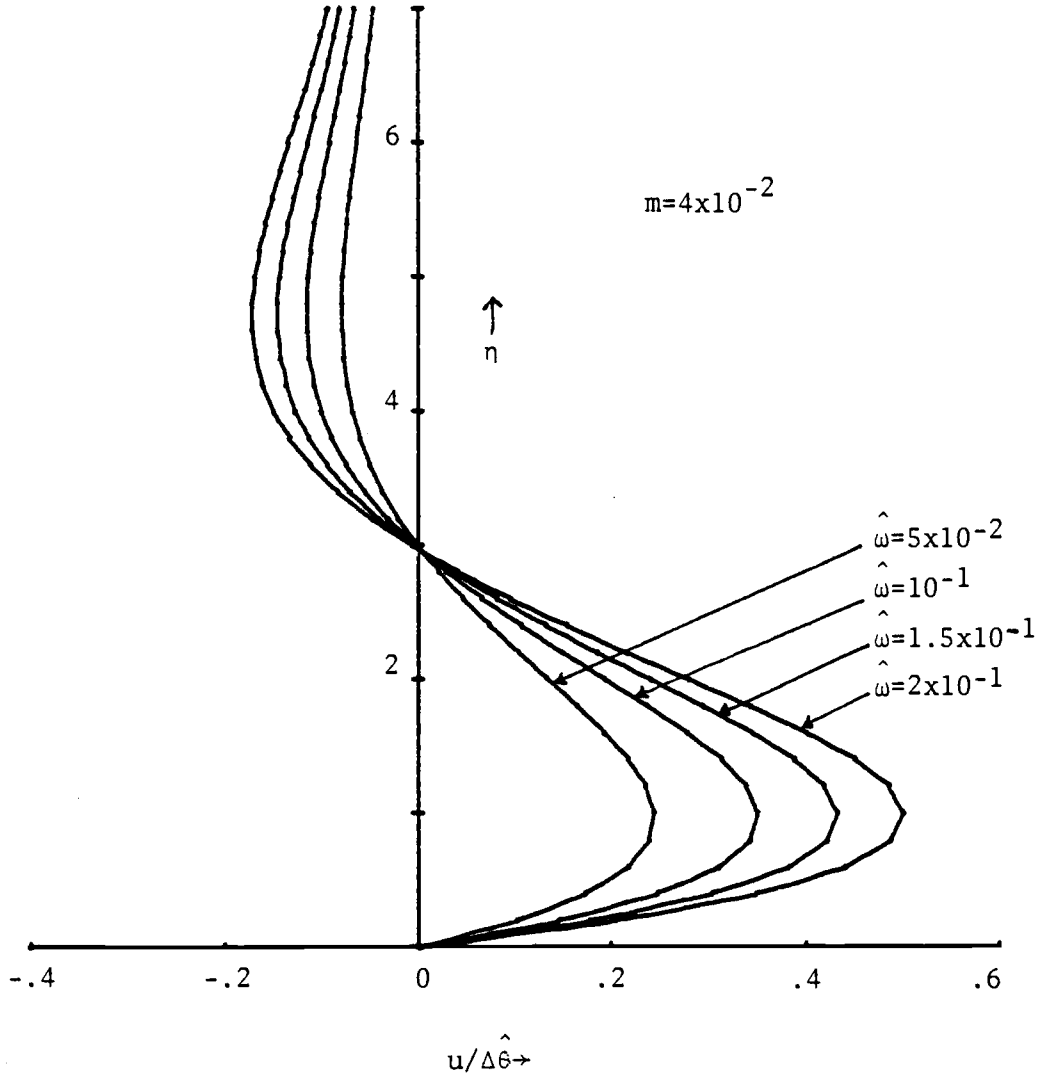

Fig. III-7-a. As in Fig. III-6-a except for several different values of $\hat{\omega}$ and $m=4\times10^{-2}$.

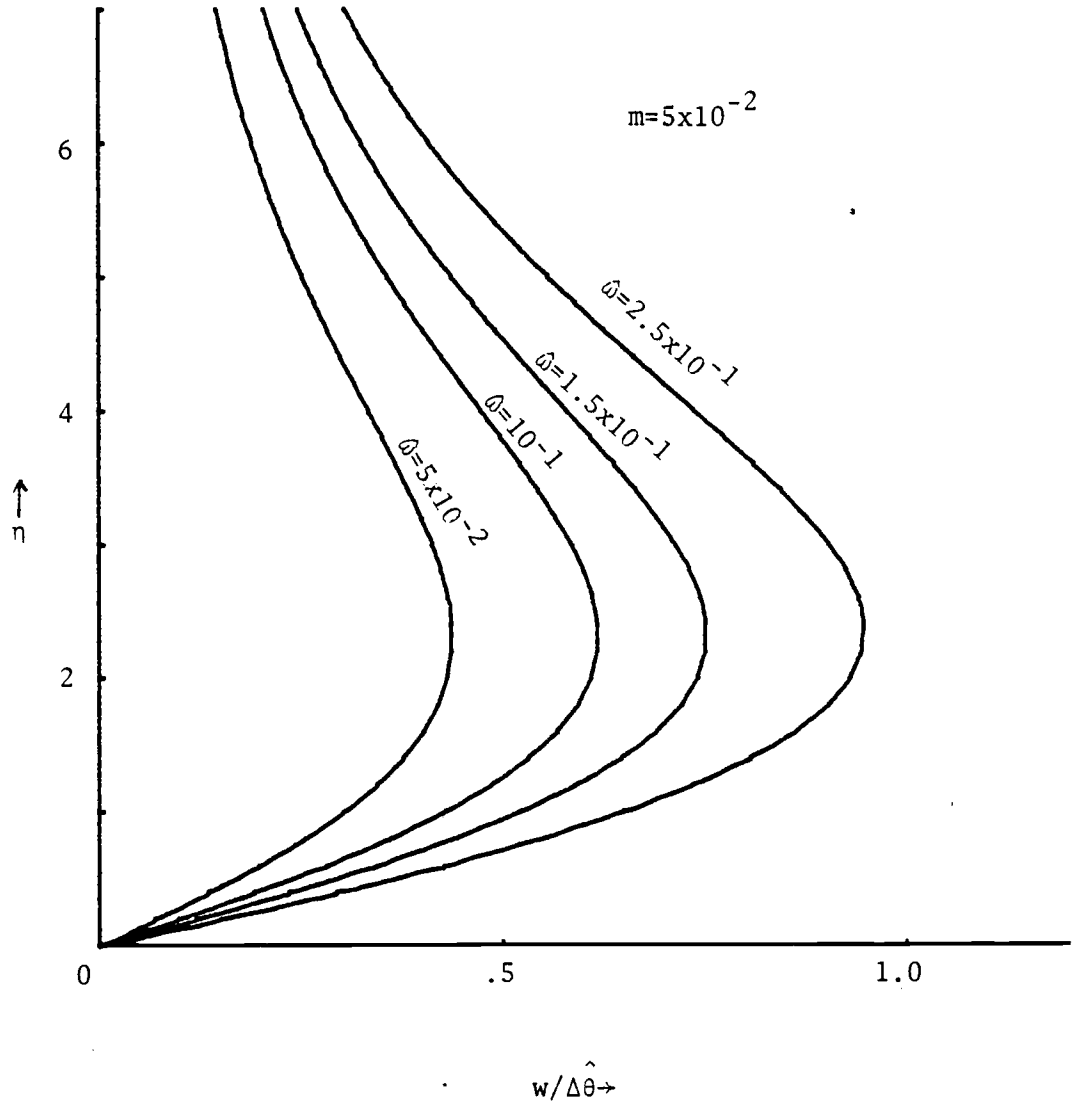

Fig. III-7-b. As in Fig. III-6-b except for several different values of $\hat{\omega}$ and $m=5\times10^{-2}$.

mid-latitudes.

The sequence obtained by the scaling of leading order terms for $\hat{\omega}<1$ is

$$\theta_S = O(1), \quad \theta_\varepsilon = O\left(\frac{m}{\sqrt{\hat{\omega}}}\right), \quad \theta_L = O\left(\frac{m}{\hat{\omega}\sqrt{\hat{\omega}}}\right)$$

$$v_S = O\left(\frac{1}{\sqrt{\hat{\omega}}}\right), \quad v_\varepsilon = O\left(\frac{1}{\sqrt{\hat{\omega}}}\right), \quad v_L = O\left(\left[\frac{m}{\hat{\omega}^3(1-\hat{\omega}^2)}\right]^{\frac{1}{2}}\right)$$

$$u_\varepsilon = O\left(\frac{1}{\sqrt{\hat{\omega}}}\right), \quad u_L = O\left(\left[\frac{m}{\hat{\omega}(1-\hat{\omega}^2)}\right]^{\frac{1}{2}}\right) \qquad \text{(III-27)}$$

$$w_\varepsilon = O\left(\frac{1}{\sqrt{\hat{\omega}}}\right), \quad w_L = O\left(\frac{1}{\sqrt{\hat{\omega}}}\right)$$

The imposed surface temperature perturbation drives the thermal Stokes layer through the thermal diffusion process as in case 2. However, the horizontal pressure gradient force induced by the horizontal temperature gradient in the thermal Stokes layer directly drives the Ekman layer without an intervening Lineykin layer.

We notice that the vertical velocity is at most $O\left(\frac{1}{\sqrt{\hat{\omega}}}\right)$ which is larger than unity. However, it is inversely proportional to the sqaure root of the imposed frequency in contrast to the case 2, where it is roughly proportional to the square root of the imposed frequency. Consequently, we expect the maximum vertical velocities at the lower frequency limit of this case, i.e. $m=\hat{\omega}^2(1-\hat{\omega}^2)$. That is, in case 2 the isallobaric contribution to the vertical motion increases with increasing frequency but further increase of $\hat{\omega}$ results in the drastic change of the governing dynamics. In case 3, the induced geostrophic wind in the thermal Stokes layer becomes weaker with increasing frequency since the depth of

the thermal wind influence decreases with increasing frequency. With higher frequencies, the thermal influence has less time to propagate before the forcing reverses sign. As a consequence of decreased thermal and geostrophic winds, the frictionally-driven vertical motion decreases with increasing frequency. As a further consequence of the small geostrophic winds, the isallobaric wind and its contribution to the vertical motion is smaller in case 3 compared to case 2. On the other hand, in the corresponding dynamically-driven flow, the vertical motion does not decrease with $\hat{\omega}$ in this region. In the dynamic case, the depths of the layers are not related to frequency through temperature diffusion (see Appendix V).

The solutions in Eqs. (III-12), (III-16) and (III-17) are determined by the application of boundary conditions at $\eta=0$ in the sequence

$$\begin{aligned} \theta_s &= \Delta\hat{\theta} \\ v_s + v_\varepsilon &= 0 \\ u_\varepsilon + u_L &= 0 \\ w_\varepsilon + w_L &= 0 \end{aligned} \qquad \text{(III-28)}$$

The total solutions are

$$p = \frac{\Delta\hat{\theta}(1+i)}{\sqrt{2\hat{\omega}}}\left[-e^{-\sqrt{\frac{\hat{\omega}}{2}}(1-i)\eta} + \sum_{j=1}^{2} C_j e^{-u_j\eta} + O\left(\left[\frac{m(1-\hat{\omega}^2)}{\hat{\omega}^2}\right]^{\frac{1}{2}}\right)\right] \qquad \text{(III-29-a)}$$

$$\theta = \Delta\hat{\theta}\left[e^{-\sqrt{\frac{\hat{\omega}}{2}}(1-i)\eta} + O\left(\frac{m}{\hat{\omega}\sqrt{\hat{\omega}}}\right)\right] \qquad \text{(III-29-b)}$$

$$v = \frac{\Delta\hat{\theta}(1+i)}{\sqrt{2\hat{\omega}}}\left[e^{-\left(\frac{\hat{\omega}}{2}\right)^{\frac{1}{2}}(1-i)\eta} + \frac{C_1}{m}\left\{\mu_1{}^2(\mu_1{}^2+i\hat{\omega})^2-m\right\}e^{-\mu_1\eta} + \frac{C_2}{m}\cdot \right.$$

$$\left. \left\{\mu_2{}^2(\mu_2{}^2+i\hat{\omega})^2-m\right\}e^{-\mu_2\eta} + O\left(\left[\frac{m}{\hat{\omega}^2(1-\hat{\omega}^2)}\right]^{\frac{1}{2}}\right)\right] \qquad \text{(III-29-c)}$$

$$u = \frac{\Delta\hat{\theta}(1+i)}{\sqrt{2\hat{\omega}}} \frac{\mu_1\mu_2}{f(\mu_1,\mu_2)}\left[\sqrt{\frac{m}{1-\hat{\omega}^2}}\, e^{-\sqrt{\frac{m}{1-\hat{\omega}^2}}\,\eta} - \frac{1}{\mu_2-\mu_1}\left\{ \mu_1\left(\mu_2-\sqrt{\frac{m}{1-\hat{\omega}^2}}\right) e^{-\mu_1\eta} \right.\right.$$

$$\left.\left. -\mu_2\left(\mu_1-\sqrt{\frac{m}{1-\hat{\omega}^2}}\right) e^{-\mu_2\eta}\right\}\right] \qquad \text{(III-29-d)}$$

$$w = \frac{\Delta\hat{\theta}(1+i)}{\sqrt{2\hat{\omega}}} \frac{\mu_1\mu_2}{f(\mu_1,\mu_2)}\left[e^{-\sqrt{\frac{m}{1-\hat{\omega}^2}}\,\eta} - \frac{1}{\mu_2-\mu_1}\left\{ \left(\mu_2-\sqrt{\frac{m}{1-\hat{\omega}^2}}\right)e^{-\mu_1\eta} \right.\right.$$

$$\left.\left. -\left(\mu_1-\sqrt{\frac{m}{1-\hat{\omega}^2}}\right) e^{-\mu_2\eta}\right\}\right] \qquad \text{(III-29-e)}$$

where

$$C_1 = \frac{m\mu_2(\mu_2{}^2 + i\hat{\omega})\left(\mu_2 - \sqrt{\frac{m}{1-\hat{\omega}^2}}\right)}{f(\mu_1,\mu_2)\ (\mu_2-\mu_1)}$$

$$C_2 = \frac{m\mu_1(\mu_1{}^2+i\hat{\omega})\left(\mu_1 - \sqrt{\frac{m}{1-\hat{\omega}^2}}\right)}{f(\mu_1,\mu_2)\ (\mu_1-\mu_2)}$$

$$C_L = -\frac{\Delta\hat{\theta}(1-i)\sqrt{m(1-\hat{\omega}^2)}}{\hat{\omega}\sqrt{2\hat{\omega}}} \cdot \frac{\mu_1\mu_2}{f(\mu_1,\mu_2)}$$

and

$$f(\mu_1,\mu_2)=(\mu_2+\mu_1)\left\{\mu_1{}^2\mu_2{}^2-m\left(\hat{\omega}i + \frac{m}{1-\hat{\omega}^2}\right)\right\} - \sqrt{\frac{m}{1-\hat{\omega}^2}}\ (\mu_1\mu_1-\hat{\omega}i-\frac{m}{1-\hat{\omega}^2})\cdot$$

$$(\mu_1\mu_2+m)$$

Profiles of cross-isobar flow Eq. (III-29-d) are presented in Figs. III-8-a and III-8-b for given values $\hat{\omega}$ and m. As both $\hat{\omega}$ and m

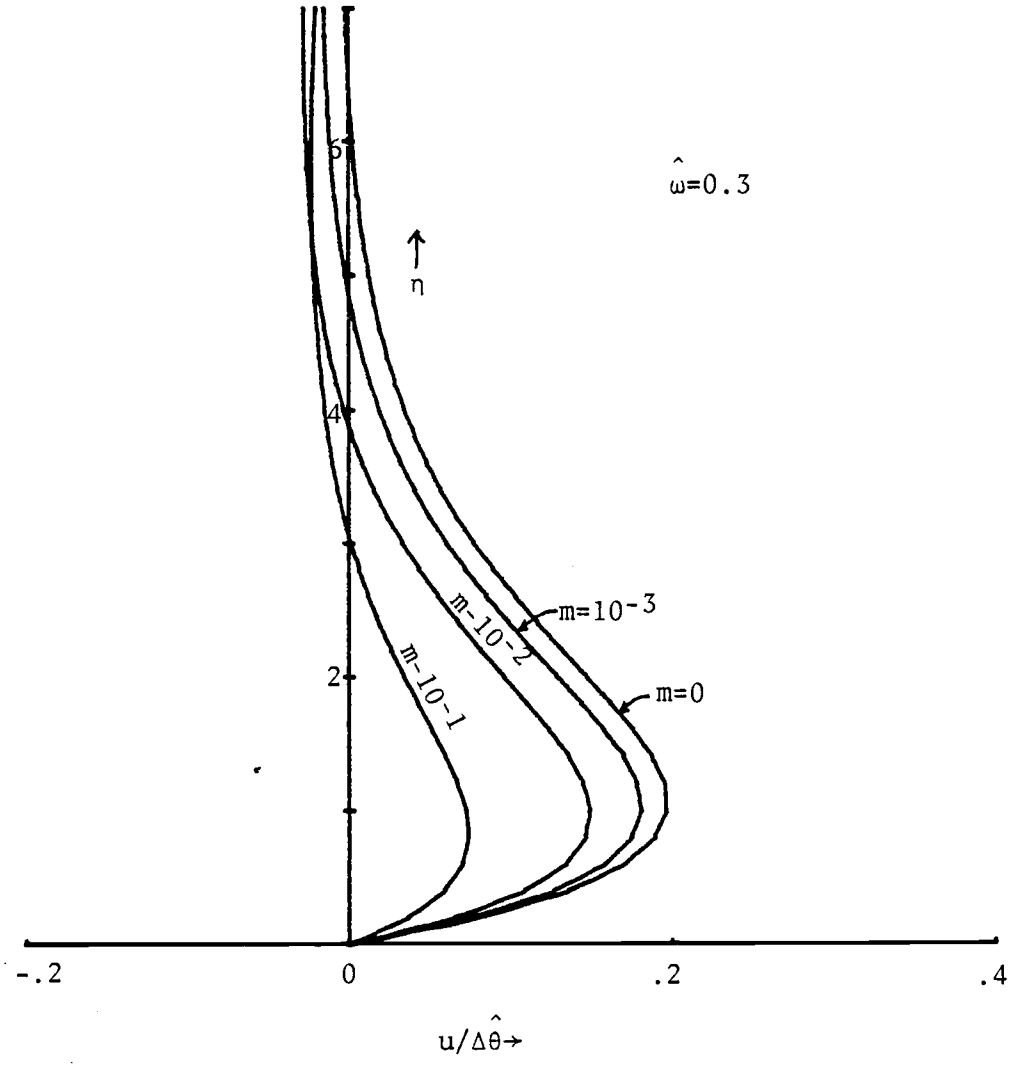

Fig. III-8-a. Scaled amplitude of the cross-isobar flow Eq. (III-29-d) as a function of height for several different values of m and $\hat{\omega}$=0.3.

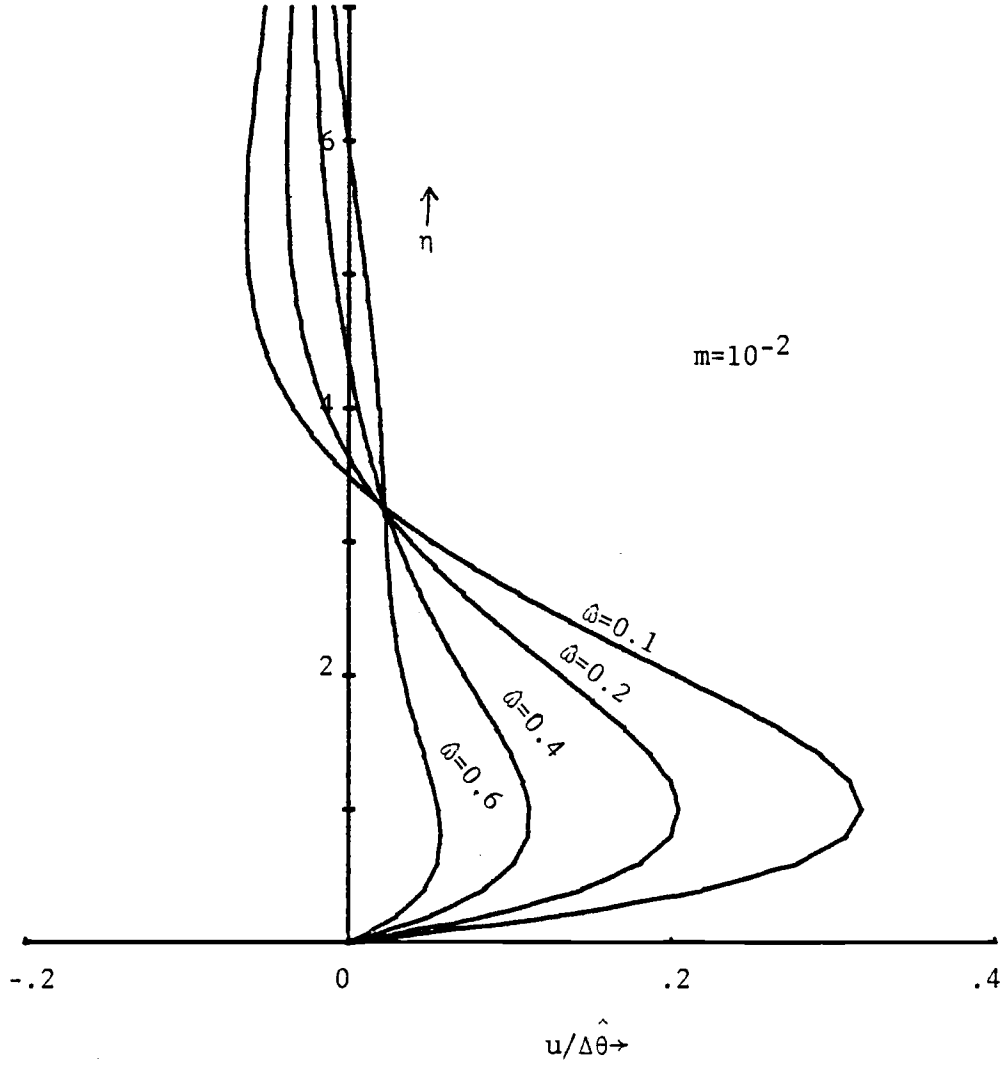

Fig. III-8-b. As in Fig. III-8-a except for several different values of ω and $m=10^{-2}$.

increase, the cross-isobar flow becomes generally weaker. The main exception is that the return cross-isobar flow above the Ekman layer increases as m increases due to pressure adjustments within the oscillatory Lineykin layer. Once again the half-width of the vertical wavelength does not change with increasing $\hat{\omega}$.

Profiles of vertical motion Eq. (III-29-e) are plotted in Figs. III-9-a and III-9-b for a given value of $\hat{\omega}$ and m. The influence of stratification on the vertical motion is similar to that described in cases 1 and 2. Even though the vertical motion is reduced throughout the whole layer with increasing $\hat{\omega}$, the reduction rate becomes smaller above the Ekman layer. Frictional effects retard accelerations in the boundary layer. The dependency of the vertical motion on m and $\hat{\omega}$ is presented in Fig. III-10 by evaluating Eq. (III-29-e) at the height $\eta=4$, where the latter is considered to be the top of the classical Ekman layer.

The geophysical applicability is more interesting in this case than in case 1 or case 2. In cases 1 and 2, the time scale is slow enough that the diffusion processes play dominant roles in the governing dynamics even far away from the boundary. However in the geophysical flow cases, the turbulent eddy diffusivities (heat or momentum) become small far away from the boundary. In case 3, the boundary layer growth or development of the thermal diffusion layer is sufficiently inhibited by oscillations that the assumption of constant eddy viscosity is less serious.

One example of the importance of surface temperature perturbations is the frequent occurrence of nocturnal thunderstorms over the

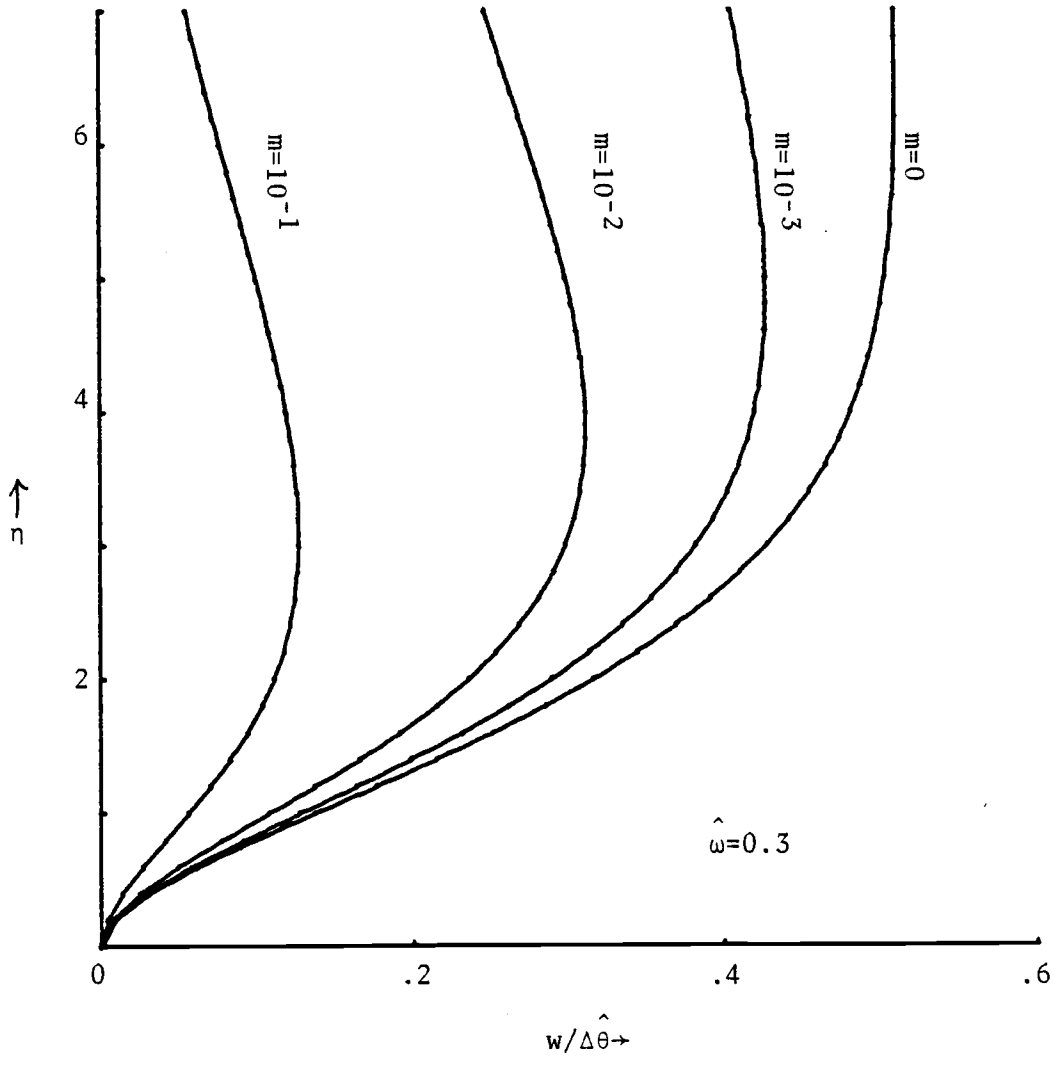

Fig. III-9-a. Scaled amplitude of the vertical velocity Eq. (III-29-e) as a function of height for several different values of m and $\hat{\omega}$=0.3.

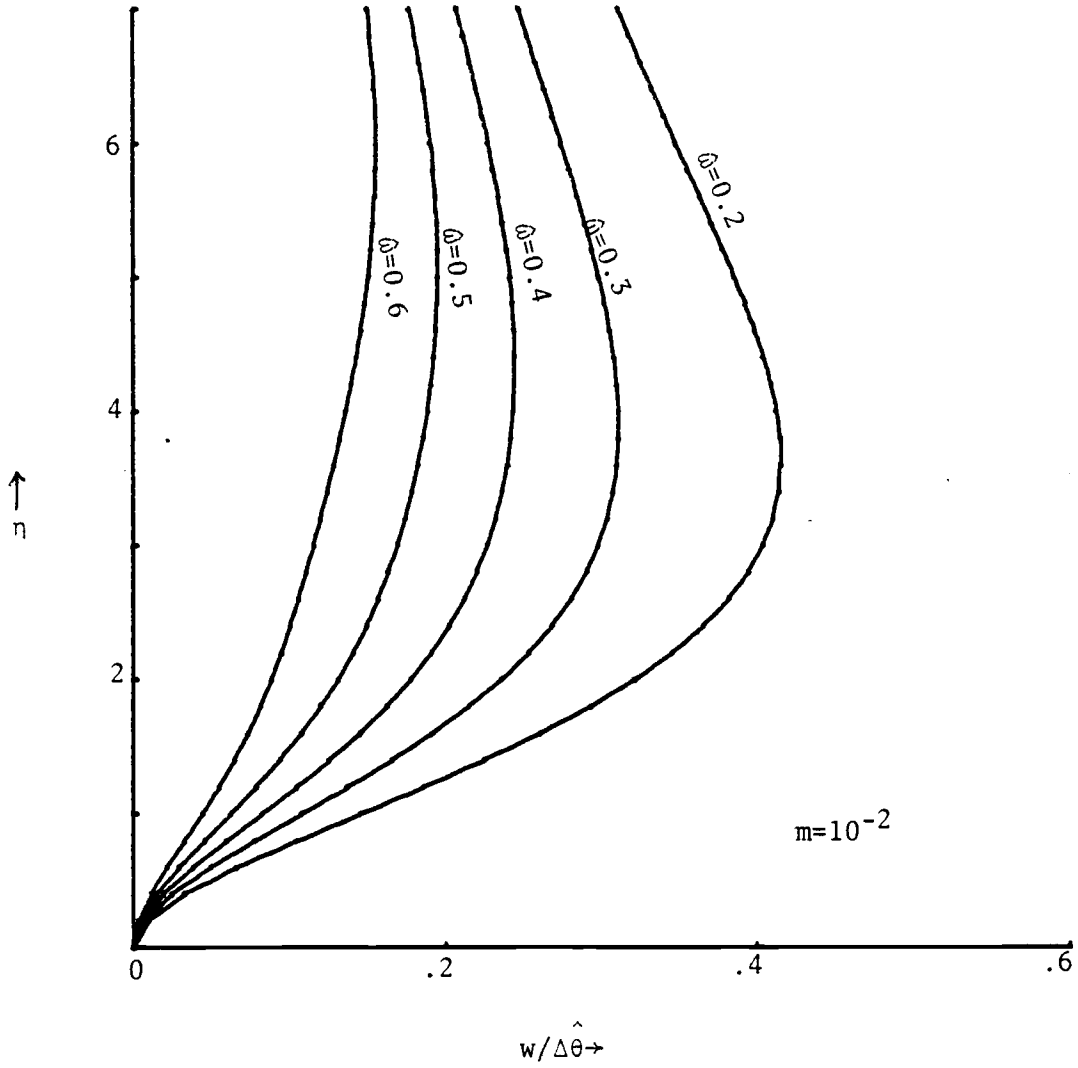

Fig. III-9-b. As in Fig. III-9-a except for several different values of ω and $m=10^{-2}$.

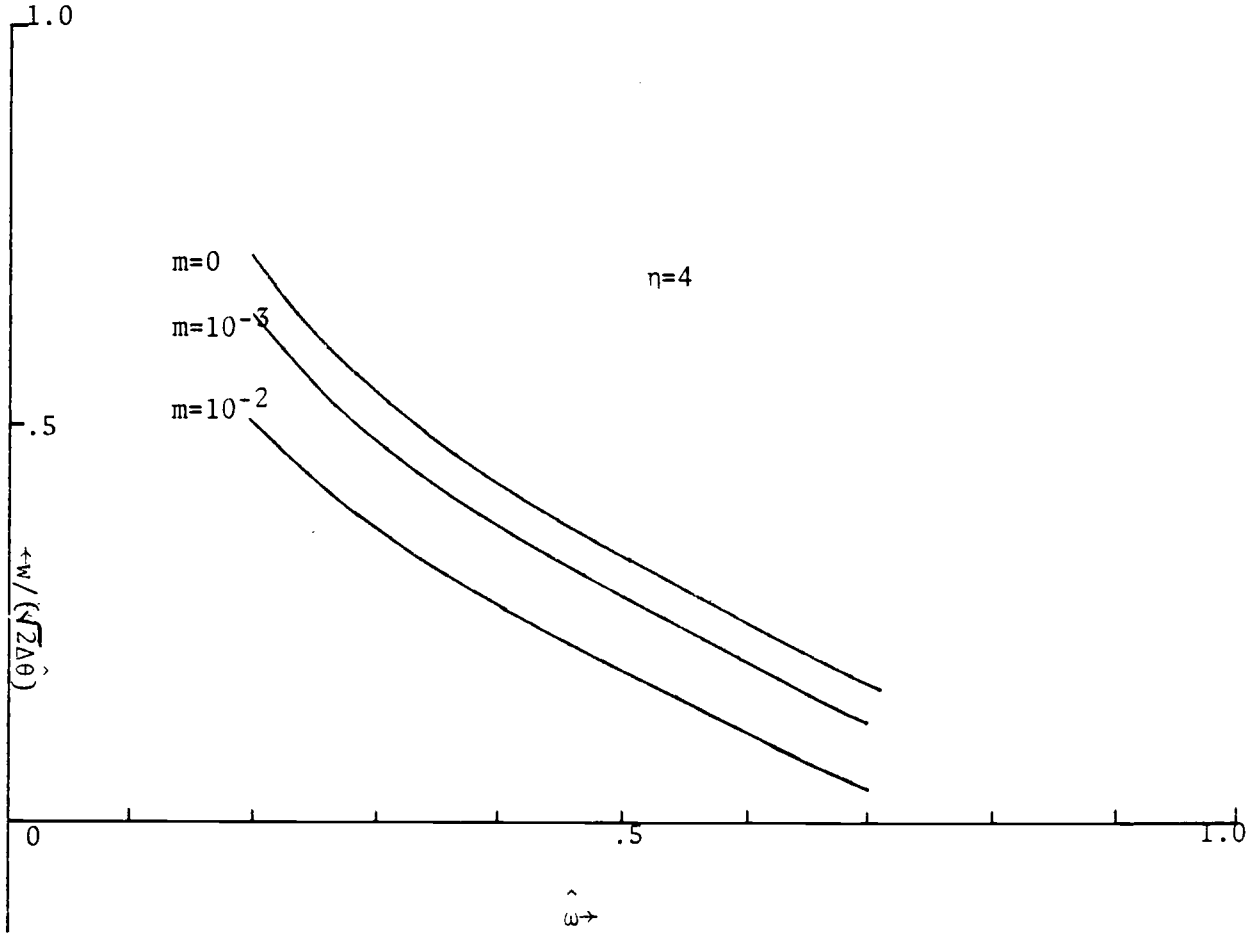

Fig. III-10. Scaled amplitude of the vertical velocity versus $\hat{\omega}$ evaluated at the top of the classical Ekman layer, η=4. Each curve represents a specific value of m.

Great Plains. The nocturnal thunderstorm is, in part, thought to be driven by large-scale, low-level baroclinity and the associated low-level jet (Bonner, 1966). However, the more detailed explanation of that phenomenon requires the introduction of the mechanical influence of the terrain slope as well as the diurnally-varying interactions between eddy diffusivities and stratification.

IV. SUMMARY AND CONCLUSIONS

The influence of prescribed boundary layer pumping on an externally-forced, synoptic-scale flow is examined in isentropic coordinates. The results indicate the following:

1) The influence of the stratification on the spin-down process is important when the externally imposed length scale is smaller than g/fN, where g is the gravitational acceleration, f is the Coriolis parameter, and N the Brunt-Väisälä frequency. In this case the vertical damping of the influence of Ekman pumping is largely concentrated in the lower troposphere. The penetration depth of boundary layer pumping is fL/N, where L is the horizontal length scale of the flow. When the imposed length scale is larger than g/fN, the influence of the stratification on the spin-down process is no longer important; instead the atmosphere responds to the Ekman pumping as a homogeneous atmosphere. However the synoptic length scale is usually less than g/fN, and boundary layer pumping can significantly alter the flow in the lower troposphere.

2) The spin-down time scale for the synoptic-scale forcing is L/FN, where F is the boundary layer pumping efficiency. The spin-down rate is proportional to the Ekman pumping efficiency and inversely proportional to the depth scale of the free flow. That is, with large pumping efficiency, more mass is pumped upward for a given-time scale, while for small free-flow depth scale, the flow is more sensitive to a given mass flux from the boundary layer.

Stratified, boundary layer flow forced by an oscillating surface temperature perturbation is examined using the order-of-magnitude scale

analysis for the case of $m \ll 1$ and $\hat{\omega} < 1$, where m is the stratification parameter multiplied by the Ekman number and $\hat{\omega}$ is the non-dimensional forcing frequency. This analysis enables us to present a picture of three distinctive types of dynamics associated with the influence of stratification and accelerations on boundary layer flow.

For $m > \hat{\omega}(1-\hat{\omega}^2)$, the oscillating Lineykin layer responds to the imposed surface temperature perturbation as if it were a steady state Lineykin layer. In particular, the dynamics of this layer is strongly controlled by the heat diffusion process, consequently the isallobaric contribution to the vertical motion is negligible. The vertical motion is principally due to frictional effects.

For $\hat{\omega}(1-\hat{\omega}^2) > m > \hat{\omega}^2(1-\hat{\omega}^2)$, the imposed surface temperature perturbation is absorbed primarily in the thermal Stokes layer through the temperature diffusion processes. The associated velocity field (or horizontal pressure gradient force) in this layer directly contributes to the isallobaric wind component in the oscillatory Lineykin layer. In the latter, the local change of temperature is more important in the thermodynamic equation than is the diffusion process. As a result stronger vertical motions are maintained.

As $\hat{\omega}$ increases so that $\hat{\omega}^2(1-\hat{\omega}^2) > m > \frac{(1-\hat{\omega}^2)^2}{\hat{\omega}}$, the depth of thermal influence induced by the imposed surface temperature perturbation in the thermal Stokes layer becomes thinner so that the associated geostrophic and vertical motion fields are weaker. This wind field directly drives Ekman pumping through frictional effects.

As $\hat{\omega}$ increases beyond $\frac{(1-\hat{\omega}^2)^2}{\hat{\omega}} > m$, the oscillatory Lineykin layer disappears and the $E^{\frac{1}{4}}$-layer assumes control of the dynamics.

As the stratification increases, the vertical motion and the cross-isobar flow are considerably reduced for all three cases discussed above. The Lineykin layer or oscillatory Lineykin becomes shallower with increasing stratification causing pressure adjustments to intensify in the lowest layers. As a result the potential convergence within the Ekman layer is largely compensated by the divergence induced by pressure adjustments. If the stratification is so strong that all the frictional convergence within the Ekman layer is completely compensated by the Lineykin divergence, the stretching of the fluid column by Ekman "suction" vanishes. However, for synoptic-scale atmospheric motion, such strong stratification seems unlikely.

The above theory is useful in predicting the possible importance and qualitative nature of the fundamental influences of accelerations and stratification on the boundary layer production of vertical motion. However, the above development cannot resolve the details of circulation development in the real atmosphere where the variations of eddy exchange coefficients with stratification and elevation above the ground are likely to be important, or where the exchange coefficient may be completely inapplicable.

BIBLIOGRAPHY

Abramowitz, M., and I. A. Stegun, 1968: Handbook of mathematical functions. Dover, 1046 pp.

Allen, J. S., 1972: Upwelling of stratified fluid in a rotating annulus: steady state. Part 1. Linear theory. J. Fluid Mech., 56, 429-445.

Barcilon, V., and J. Pedlosky, 1967a: Linear theory of rotating stratified fluid motion. J. Fluid Mech., 29, 1-16.

_____, and _____, 1967b: A unified theory of homogeneous and stratified rotating fluids. J. Fluid Mech., 29, 609-621.

Bergstrom, R. W., and A. C. Cogley, 1976: Viscous boundary layers in rotating fluids driven by periodic flows. J. Atmos. Sci., 33, 1234-1247.

Bleck, R., 1973: Numerical forecasting experiments based on the conservation of potential vorticity on isentropic surfaces. J. Appl. Meteor., 12, 737-752.

Blumsack, S., and A. Barcilon, 1971: Thermally-driven linear vortex. J. Fluid Mech., 48, 801-814.

_____, P. J. Gierasch, and W. R. Wessel, 1973: An analytical and numerical study of the Martian planetary boundary layer over slopes. J. Atmos. Sci., 30, 66-79.

Bonner, W. D., 1966: Case study of thunderstorm activity in relation to the low-level jet. Mon. Wea. Rev., 94, 167-178.

Buajitti, K., and A. Blackadar, 1957: Theoretical studies of diurnal wind variations in the planetary boundary layer. Quart. J. Roy. Met. Soc., 83, 486-500.

Buzyna, C., and G. Veronis, 1971: Spin-down of a stratified fluid: Theory and experiment. J. Fluid Mech., 50, 579-608.

Calder, K. L., 1968: In clarification of the equations of shallow-layer thermal convection for a compressible fluid based on the Boussinesq approximation. Quart. J. Roy. Met. Soc., 94, 88-92.

Charney, J. G., and A. Eliassen, 1949: A numerical method of predicting the perturbations of the middle latitude westerlies. Tellus, 1, 38-54.

_____, and M. Stern, 1962: On the stability of internal baroclinic jets in a rotating atmosphere. J. Atmos. Sci., 19, 159-172.

Chervin, R. M., and S. H. Schneider, 1976: On determining the statistical significance of climate experiments with general circulation models. J. Atmos. Sci., 33, 405-412.

Cogley, A. C., 1976: Circularly polarized inertial wave vectors in rotating fluids. J. Atmos. Sci., 33, 1023-1233.

Estoque, M. A., 1963: A numerical model of the atmospheric boundary layer. J. Geophys. Research, 68, 1103-1113.

Gates, W. L., 1961: Static stability measures in the atmosphere. J. Meteor., 18, 526-533.

Goody, R. M., 1953: Equations of transfer for the total flux of terrestrial radiation. Quart. J. Roy. Met. Soc.,79, 282-283.

_____, 1960: The influence of radiative transfer on the propagation of a temperature wave in a stratified diffusing atmosphere. J. Fluid Mech., 9, 445-454.

Greenspan, H. P., and L. N. Howard, 1963: On the time-dependent motion of a rotating fluid. J. Fluid Mech., 17, 385-404.

Haltiner, G. J., 1971: Numerical Weather Prediction. Wiley, 317 pp.

Holton, J. R., 1965: The influence of viscous boundary layers on transient motions in a stratified rotating fluid. Part I. J. Atmos. Sci., 22, 402-411.

_____, 1967: The diurnal boundary layer wind oscillation above sloping terrain. Tellus, 19, 199-205.

Houghton, D. D., J. E. Kutzbach, M. McClintock, and D. Suchman, 1974: Response of a general circulation model to a sea temperature perturbation. J. Atmos. Sci., 31, 857-868.

Kestin, J., P. F. Maeder, and H. E. Wang, 1960: On boundary layers associated with oscillating streams. Appl. Sci. Res., 10, 1-22.

Kondrat'yev, K. Y., 1965: Actinometry. NASA TT F-9712, 675 pp.

Krishna, K., 1968: A numerical study of the diurnal variation of Meteorological parameters in the Planetary boundary layer: Part I, diurnal variations of winds. Mon. Wea. Rev., 96, 269-276.

Kuo, H. L., 1973: Planetary boundary layer flow of a stable atmosphere over the globe. J. Atmos. Sci., 30, 53-65.

___, 1975: Planetary boundary layer of equatorial waves and critical latitude. Bound. Layer Meteor., 9, 163-190.

Leetmaa, A., 1971: Some effects of stratification on rotating fluids. J. Atmos. Sci., 28, 65-71.

Lighthill, M. J., 1954: The response of laminar skin friction and heat transfer to fluctuations in the stream velocity. Proc. Roy. Soc. London, A224, 1-23.

Lineykin, Q. S., 1955: On the determination of the thickness of the baroclinic layer in the sea. Doklady SSSR Adad. Nauk, Tom 101, 461-464.

Lykosov, V. N., 1972: Unsteady state in the planetary boundary layer of the atmosphere. Acad. Sci. USSR, Atmos. and Oce. Phys., 8, 85-91.

Mahrt, L. J., 1974: Time-dependent integrated planetary boundary layer flow. J. Atmos. Sci., 31, 457-464.

_____, 1975: The influence of momentum advections on a well-mixed layer. Quart. J. Roy. Met. Soc., 101, 1-11.

Mak, M. K., 1974: On the frequency dependence and dynamics of accelerating neutral planetary boundary layer. J. Atmos. Sci., 31, 475-482.

Namias, J., 1976: Negative ocean-air feedback systems over the North Pacific in the transition from warm to cold seasons. Mon. Wea. Rev., 104, 1107-1121.

Paegle, J., 1970: Studies of diurnally periodic boundary layer wind. Technical Report, NSF Grant GA-698, Dept. of Meteorology, UCLA 69 pp.

_____, and G. E. Rasch, 1973: Three-dimensional characteristics of diurnally varying boundary-layer flows, Mon. Wea. Rev., 101, 746-756.

Phillips, N. A., 1963: Geostrophic motion. Rev. Geophys., 1, 123-176.

Sakurai, T., 1969: Spin-down problem of rotating stratified fluid in thermally insulated circular cylinders. J. Fluid Mech., 37, 689-699.

Spar, J., 1973: Some effects of surface anomalies in a global general circulation model. Mon. Wea. Rev., 701, 91-100.

Spiegal, E. A., and G. Veronis, 1960: On the Boussinesq approximation for a compressible fluid. Astrophys. J., 131, 442-447.

APPENDICES

APPENDIX I

Quasi-geostrophic Potential Vorticity Equations

The results of linearized quasi-geostrophic potential vorticity equations derived in each coordinate system are given by

$$\frac{\partial}{\partial t}\left[\nabla^2 p_o + \frac{\partial}{\partial z}\left\{\left(-\frac{d\rho_s^o}{dz} B^2\right)\frac{\partial p_o}{\partial z}\right\}\right] = 0 \qquad \text{(A-I-1)}$$

$$\frac{\partial}{\partial t}\left[\nabla^2 \phi_o + \frac{1}{\mathfrak{P}}\frac{\partial}{\partial Z}\left(\frac{\mathfrak{P}}{R_o^2 R_i}\frac{\partial}{\partial Z}\right)\phi_o\right] = 0 \qquad \text{(A-I-2)}$$

$$\frac{\partial}{\partial t}\left[\nabla^2 \phi_o + \frac{\partial}{\partial p}\left(\frac{1}{S_N^2}\frac{\partial \phi_o}{\partial p}\right)\right] = 0 \qquad \text{(A-I-3)}$$

$$\frac{\partial}{\partial t}\left[\nabla^2 M_o + \left\{B'\left(1 + \frac{\Delta\theta}{\theta_o}\theta\right)\right\}^2 \frac{\partial^2 M_o}{\partial \theta^2}\right] = 0 \qquad \text{(A-I-4)}$$

where the subscribed "o" represents the zero order field variable expanded in terms of powers of the inverse time scale

$$B^2 \equiv \frac{Q_{sg}}{\rho_o L f^2} \quad , \quad B' = \frac{NfL\theta_o}{g\Delta\theta}$$

$$\mathfrak{P} \equiv \frac{p}{p_{oo}}$$

$$Z = -\ell n\ p$$

$$R_o \equiv \frac{U}{fL}$$

$$R_i \equiv \frac{1}{U^2}\frac{\partial}{\partial Z}\left(\frac{\partial \phi_s}{\partial Z} + \kappa\phi_s\right)$$

$$p_{oo} = 1000\text{mb}$$

and Q_s is the scale of basic state density

ϕ_s is the basic state geopotential height

$\overline{S}_N \equiv - \frac{\overline{\alpha}}{\overline{\theta}} \frac{\partial \overline{\theta}}{\partial p}$, bar quantities are mean basic state

All quantities in Eq. (A-1-4) are defined in the text. Eq. (A-I-1) is derived in z-coordinates (Walin, 1969), (A-I-2) in log pressure coordinates (Phillips, 1963), (A-I-3) in pressure coordinates (Haltiner, 1971) and (A-I-4) in isentropic coordinates.

APPENDIX II

Governing Equations for the Stratified Boundary Layer

We employ the Cartesian coordinate system (x,y,z) in the conventional manner with x increasing eastward, y increasing northward and z increasing upward. Since our interest is to investigate secondary flows set up in the atmosphere by boundary forcing, it is convenient to treat the departures p_*', ρ_*', θ_*', T_*' of the pressure, density, potential temperature and temperature from their basic state values p_o, ρ_o, θ_o, T_o (which are functions of z only) as small quantities, i.e.,

$$\frac{p_*'}{p_o}, \frac{\theta_*'}{\theta_o}, \frac{T_*'}{T_o}, \frac{\rho_*'}{\rho_o} \ll 1.$$

The equations of motion, the thermodynamic equation and the continuity equation with Boussinesq approximation can then be written as (e.g. Spiegel and Veronis, 1960; Calder, 1968; Kuo, 1973)

$$\frac{\partial \vec{v}_*}{\partial t} + \vec{v}_* \cdot \vec{\nabla}\vec{v}_* + f\vec{k}x\vec{v}_* = -\frac{1}{\rho_o}\vec{\nabla}p_*' + \frac{\theta_*'}{\theta_o} g\vec{k} + \vec{\nabla}\cdot(k\vec{\nabla}\cdot\vec{v}_*) \quad \text{(A-II-1)}$$

$$\frac{\partial \theta_*'}{\partial t} + \vec{v}_*\cdot\vec{\nabla}\theta_*' + w_*\frac{\partial \theta_s}{\partial z} = \vec{\nabla}\cdot(k_H\nabla\theta_*') + Q_R \quad \text{(A-II-2)}$$

$$\vec{\nabla}\cdot\vec{v}_* = 0 \quad \text{(A-II-3)}$$

where $\vec{v}_*$ is the velocity vector with components (u_*,v_*,w_*) in the respective directions (x,y,z), $\vec{k}$ is the unit vector in the z direction, Q_R is radiational heating or cooling rate per unit mass, and the differential operator $\vec{\nabla} = \frac{\partial}{\partial x}\vec{i} + \frac{\partial}{\partial y}\vec{j} + \frac{\partial}{\partial z}\vec{k}$. Since we are seeking physical

insight into the fundamental interactions between turbulent scales and comparatively large scales of flow, a relatively simple parameterization of turbulent transports is sufficient. In this study we adopt a constant eddy viscosity K and a constant thermal eddy viscosity K_H to approximate the influence of turbulent transports. Furthermore, we explicitly neglect the radiational heating or cooling term $Q_R = 0$ (see Appendix III).

We introduce nondimensional variables such that

$$
\begin{aligned}
(u_*, v_*, w_*) &= V(\hat{u}, \hat{v}, \frac{H}{L}\hat{w}) \\
(x, y) &= L(\hat{x}, \hat{y}) \\
z &= H\hat{z} \\
p_*' &= fLVp_S\hat{p} \\
\frac{\theta_*'}{\theta_o} &= \frac{fLV}{gH}\hat{\theta}\ , \quad t = \omega^{-1}\hat{t}
\end{aligned}
\qquad \text{(A-II-4)}
$$

where V is the characteristic velocity, L is the scale of variation of the horizontal direction, H is the scale height, the scale of p_*' is chosen by balancing the Coriolis force and pressure gradient terms, and the scale for θ_*' is determined from hydrostatic balance and the Boussinesq approximation. ω is the forcing frequency.

Scaling Eqs. (A-II-1) - (A-II-3) with Eq. (A-II-4) we obtain the following nondimensional equations:

$$
\hat{\omega}\frac{\partial\hat{u}}{\partial\hat{t}} + R_o\left(\hat{u}\frac{\partial\hat{u}}{\partial\hat{x}} + \hat{v}\frac{\partial\hat{u}}{\partial\hat{y}} + \hat{w}\frac{\partial\hat{u}}{\partial\hat{z}}\right) - \hat{v} = -\frac{\partial\hat{p}}{\partial\hat{x}} + E\left(\frac{\partial^2\hat{u}}{\partial\hat{z}^2} + \left(\frac{H}{L}\right)^2\nabla_H^2\hat{u}\right)
\qquad \text{(A-II-5)}
$$

$$\hat{\omega}\frac{\partial\hat{v}}{\partial\hat{t}} + R_o\left(\hat{u}\frac{\partial\hat{v}}{\partial\hat{x}} + \hat{v}\frac{\partial\hat{v}}{\partial\hat{y}} + \hat{w}\frac{\partial\hat{v}}{\partial\hat{z}}\right) + \hat{u} = -\frac{\partial\hat{p}}{\partial\hat{y}} + E\left(\frac{\partial^2\hat{v}}{\partial\hat{z}^2} + \left(\frac{H}{L}\right)^2 \nabla_H{}^2\hat{v}\right) \tag{A-II-6}$$

$$\left(\frac{H}{L}\right)^2\left[\hat{\omega}\frac{\partial\hat{w}}{\partial\hat{t}} + R_o\left(\hat{u}\frac{\partial\hat{w}}{\partial\hat{x}} + \hat{v}\frac{\partial\hat{w}}{\partial\hat{y}} + \hat{w}\frac{\partial\hat{w}}{\partial\hat{z}}\right)\right] + \frac{\partial\hat{p}}{\partial\hat{z}} - \hat{\theta} = \left(\frac{H}{L}\right)^2 E \cdot \left(\frac{\partial^2\hat{w}}{\partial\hat{z}^2} + \left(\frac{H}{L}\right)^2 \nabla_H{}^2\hat{w}\right) \tag{A-II-7}$$

$$\hat{\omega}\frac{\partial\hat{\theta}}{\partial\hat{t}} + R_o\left(\hat{u}\frac{\partial\hat{\theta}}{\partial\hat{x}} + \hat{v}\frac{\partial\hat{\theta}}{\partial\hat{y}} + \hat{w}\frac{\partial\hat{\theta}}{\partial\hat{z}}\right) + B^2\hat{w} = \frac{E}{P_r}\left(\frac{\partial^2\hat{\theta}}{\partial\hat{z}^2} + \left(\frac{H}{L}\right)^2 \nabla_H{}^2\hat{\theta}\right) \tag{A-II-8}$$

$$\frac{\partial\hat{u}}{\partial\hat{x}} + \frac{\partial\hat{v}}{\partial\hat{y}} + \frac{\partial\hat{w}}{\partial\hat{z}} = 0 \tag{A-II-9}$$

where $\hat{\omega} \equiv \frac{\omega}{f} \equiv$ nondimensional frequency

$R_o \equiv \frac{V}{fL} \equiv$ Rossby number

$E \equiv \frac{K}{fH^2} \equiv$ turbulent Ekman number

$\frac{H}{L} \equiv$ aspect ratio

$B^2 \equiv \left(\frac{NH}{fL}\right)^2 \equiv$ stratification parameter

$N \equiv \left(\frac{g}{\theta_o}\frac{\partial\theta_o}{\partial z}\right)^{\frac{1}{2}} \equiv$ Brunt-Väisälä frequency

$f \equiv$ Coriolis parameter, assumed constant

$P_r \equiv \frac{K}{K_H} \equiv$ turbulent Prandtl number

Dropping the "^" notation and assuming $R_o << 1$, $\frac{H}{L} << 1$, $p_r = 1$, Eqs. (A-II-5)-(A-II-9) become

$$\hat{\omega}\,\frac{\partial u}{\partial t} - v = -\frac{\partial p}{\partial x} + E\,\frac{\partial^2 u}{\partial z^2} \qquad \text{(A-II-10)}$$

$$\hat{\omega}\,\frac{\partial v}{\partial t} + u = -\frac{\partial p}{\partial y} + E\,\frac{\partial^2 v}{\partial z^2} \qquad \text{(A-II-11)}$$

$$\frac{\partial p}{\partial z} = \theta \qquad \text{(A-II-12)}$$

$$\hat{\omega}\,\frac{\partial \theta}{\partial t} + B^2 w = E\,\frac{\partial^2 \theta}{\partial z^2} \qquad \text{(A-II-13)}$$

$$\frac{\partial u}{\partial x} + \frac{\partial v}{\partial y} + \frac{\partial w}{\partial z} = 0 \qquad \text{(A-II-14)}$$

We assign $E \ll 1$ but assume a boundary layer exists so that we expect $E\,\frac{\partial^2}{\partial z^2} \simeq O(1)$ in the boundary layer.

APPENDIX III

Parameterization of Radiation

The radiation transfer processes in the real atmosphere are very complicated since the atmosphere is highly selective and far from a theoretical grey atmosphere. However, a brief consideration of radiational effects is worthwhile because we will consider the boundary layer flows driven by surface heating or cooling in a manner of a perturbation temperature specified at the surface. For example Holton (1967) showed that the radiational effect can contribute substantially to the amplitude of the diurnal wind oscillation over sloping terrain.

For our purpose we utilize the approximate transfer equations. The radiative flux divergence for the horizontally uniform atmosphere may be approximated by

$$Q_R = \frac{1}{\rho C_p} \left(\frac{p_{oo}}{p}\right)^{\kappa} \frac{d}{dz}\left[S \cos \chi - \sum_{\lambda}^{\infty}(U_\lambda - G_\lambda)\right]$$

where S is the solar radiation (short wave radiation), χ is the solar zenith angle, ρ is the air density, p_{oo}=1000mb, p is pressure, U_λ and G_λ are respectively the upward and downward terrestrial radiative flux centered at the wavelength λ. In the planetary boundary layer we may assume $p \approx p_{oo}$ and that the direct absorption of solar radiation is negligible in the absence of boundary layer clouds. In this case the above equation is simplified

$$Q_R = -\frac{1}{\rho C_p} \frac{d}{dz}\left[\sum_{\lambda}^{\infty}(U_\lambda - G_\lambda)\right] = -\frac{1}{\rho C_p} \sum_{\lambda}^{\infty} \frac{dF_\lambda}{dz}$$

where F_λ is the net upward terrestrial flux at the wavelength λ. There-

fore the radiational effect can be approximated by the estimation of net flux divergence of terrestrial radiation in the boundary layer. Here U_λ, G_λ satisfy the approximate transfer equation (Kondra'yev, 1965, p. 478) such that

$$\frac{dU_\lambda}{dz} = -a_\lambda(U_\lambda - B_\lambda) \tag{A-III-1}$$

$$\frac{dG_\lambda}{dz} = a_\lambda(G_\lambda - B_\lambda) \tag{A-III-2}$$

where a_λ is the volume absorption coefficient for wavelength λ and B_λ is the Plank function (source term). Combining Eqs. (A-III-1) and (A-III-2) we obtain a single equation in terms of the net flux F_λ

$$\frac{d^2F_\lambda}{dz^2} - \frac{1}{a_\lambda}\frac{da_\lambda}{dz}\frac{dF_\lambda}{dz} - a_\lambda{}^2F_\lambda = 2a_\lambda\frac{dB_\lambda}{dz} \tag{A-III-3}$$

Eq. (A-III-3) is the same as the transfer equation derived by Goody (1953). We may assume the change of absorption coefficient with height in the planetary boundary layer is negligibly small. In which case Eq. (A-III-3) becomes

$$\frac{d^2F_\lambda}{dz^2} - a_\lambda{}^2F_\lambda = 2a_\lambda\frac{dB_\lambda}{dz} \tag{A-III-4}$$

Since the atmospheric absorption depends largely upon wavelength, we define the average absorption coefficient, a, to be (Goody, 1953)

$$a = \frac{\int_0^\infty a_\lambda\frac{dB_\lambda}{dz}\,d\lambda}{\int_0^\infty\frac{dB_\lambda}{dz}\,d\lambda}$$

For our convenience we consider two extreme groups based on the com-

parison of the mean free path of a photon and the local boundary layer thickness. One is the strongly absorbed group, and the other is the weakly absorbed group. Introducing mean absorption coefficients a_s, a_w for strongly and weakly absorbed groups, respectively, we obtain from Eq. (A-III-4)

$$\frac{d^2F_s}{dz^2} - a_s{}^2F_s = 2a_s \frac{dB_s}{dz}$$

$$\frac{d^2F_w}{dz^2} - a_w{}^2F_w = 2a_w \frac{dB_w}{dz}$$

For the strongly absorbed group, i.e. $a_s >> \frac{d}{dz}$,

$$F_s = -\frac{2}{a_s}\frac{dB_s}{dz} = -\frac{2}{a_s}\frac{d}{dz}(\alpha\sigma T^4) \simeq -\rho C_p K_R \frac{d\theta}{dz}$$

where α is the fraction of black body radiation contained in the strongly absorbed group, σ is the Stefan-Boltzmann constant and $K_R = \frac{8\alpha\sigma\theta_o{}^3}{\rho C_p a_s}$ is a radiational diffusion coefficient, and θ_o is assumed to be constant in the boundary layer. For the strongly absorbed group, a photon travels several mean free paths before escaping from the boundary layer; therefore the temperature smoothing proceeds differentially. For the weakly absorbed group, i.e. $a_w << \frac{d}{dz}$

$$\frac{d^2F_w}{dz^2} \simeq 2a_w \frac{dB_w}{dz} \simeq 8(1-\alpha)\sigma\theta_o{}^3 a_w \frac{d\theta}{dz}$$

By integration we get flux divergence

$$\frac{dF_w}{dz} = \frac{\rho C_p}{A_R}\theta$$

where $A_R = \frac{\rho C_p}{8(1-\alpha)\sigma\theta_o^3 a_w}$ which is a radiative relaxation time constant. For the weakly absorbed group, the boundary layer is optically so thin that the temperature smoothing proceeds almost entirely through emission losses.

We notice that the influence of the flux of terrestrial radiation within the boundary layer is a pure Newtonian cooling due to the weakly absorbed group, while the strongly absorbed group merely modifies the eddy heat exchange coefficient.

For a numerical example, with $\sigma=5.75\times10^{-5}$ erg cm^{-2} sec^{-1} $^oK^{-4}$, if we take $\rho C_p=10^{-4}$ erg cm^{-3} $^oK^{-1}$, $\theta_o=300^oK$, $a_w=0.5\sim4\times10^{-6}$ cm^{-1} which corresponds to a water vapor content of about 7-20 g/m^3 (Goody, 1960), $a_s=10^{-4}$ cm^{-1} and $\alpha=0.5$; then $K_R=0.4$m^2 sec^{-1} and $A_R=5\sim10$ days.

Holton (1967), in his study of diurnal oscillations of the boundary layer wind, has chosen a_w (in his parameter $\tilde{\alpha}$) = 10^{-4} cm^{-1} to make the nondimensional relaxation time scale be O(1), even though his boundary layer thickness is essentially that of the Ekman boundary layer. His value is overestimated to apply the temperature smoothing due to the Newtonian cooling effect. The above study shows that his boundary layer thickness should be less than 100m for the Newtonian cooling to be comparable to the diffusive temperature smoothing. Such a possibility is inconsistant with his numerical example where the boundary layer was much thicker.

The above examination of the radiational effect shows that for the diurnally-varying flow, the Newtonian cooling effect is too slow to be of significance. However, when the boundary layer is optically very thick the radiational diffusive process is important for the modifica-

tion of the temperature in the boundary layer.

APPENDIX IV

Solution of Cubic Equation

From Eq. (III-9), we get

$$r^3 + 2\hat{\omega}ir^2 + (1-\hat{\omega}^2)r - m = 0 \qquad \text{(A-IV-1)}$$

where $r=\alpha_i{}^2$. The cubic equation (A-IV-1) is to be solved with the restrictions of parameters ; $m<<(1-\hat{\omega}^2)^{3/2}$ and $m\hat{\omega}<<(1-\hat{\omega}^2)^2$. These restrictions correspond to the flow regimes II-a, II-b and IV in Fig. III-1.

Introducing a new variable β such that $r=\beta-\frac{2\hat{\omega}}{3}i$, we obtain a reduced cubic equation

$$f(\beta) = \beta^3 + (1+\frac{\hat{\omega}^2}{3})\beta - \left[m + \frac{2\hat{\omega}}{3}i(1-\frac{\hat{\omega}^2}{9})\right] = 0 \qquad \text{(A-IV-2)}$$

From Table 1, we can guess one approximate root

$$\tilde{\beta}_o = \frac{m}{1-\hat{\omega}^2} + \frac{2\hat{\omega}}{3}i \qquad \text{(A-IV-3)}$$

Using Newton's method (see for example Abramowitz and Stegun, 1968, p. 20) we get $\beta_o \simeq \tilde{\beta}_o - \frac{f(\tilde{\beta}_o)}{f'(\tilde{\beta}_o)}$

where

$$f(\tilde{\beta}_o) = \left(\frac{m}{1-\hat{\omega}^2}\right)^3 + 2\hat{\omega}i\left(\frac{m}{1-\hat{\omega}^2}\right)^2$$

$$f'(\tilde{\beta}_o) = (1-\hat{\omega}^2)\left[1 + 4i\frac{m\hat{\omega}}{(1-\hat{\omega}^2)^2} + 3\frac{m^2}{(1-\hat{\omega}^2)^3}\right]$$

Since $m\hat{\omega}<<(1-\hat{\omega}^2)^2$ and $m<<(1-\hat{\omega}^2)^{3/2}$, we get

$$\beta_o \simeq \frac{m}{1-\hat{\omega}^2} + \frac{2\hat{\omega}}{3} i - \frac{m^2}{(1-\hat{\omega}^2)^4} \left[2\hat{\omega}(1-\hat{\omega}^2)i + m\right] \qquad \text{(A-IV-4)}$$

If $m>\hat{\omega}(1-\hat{\omega}^2)$ which corresponds to case 1 in Sec. III, we get

$$\beta_o \simeq \frac{m}{1-\hat{\omega}^2}(1-\beta') + \frac{2\hat{\omega}}{3} i$$

where $\beta' = \frac{m^2}{(1-\hat{\omega}^2)^3} << 1$. The other two roots are obtained by dividing $f(\beta)$ by $\beta-\beta_o$. The three roots of Eq. (A-IV-1) are

$$r_o \simeq \frac{m}{1-\hat{\omega}^2}(1-\beta')$$

$$r_{1,2} \simeq -\frac{m(1-\beta')}{2(1-\hat{\omega}^2)} - \left(\hat{\omega} \pm \sqrt{1+\beta'}\right) i \qquad \text{(A-IV-5)}$$

If $m<\hat{\omega}(1-\hat{\omega}^2)$, corresponding to the case 2 and 3 in Sec. III, we obtain

$$\beta_o \simeq \frac{m}{1-\hat{\omega}^2}(1-\beta''i)$$

where $\beta'' = \frac{2m\hat{\omega}}{(1-\hat{\omega}^2)^2} << 1$

The roots are then

$$r_o \simeq \frac{m}{1-\hat{\omega}^2}(1-\beta''i)$$

$$r_{1,2} \simeq -\frac{m}{2(1-\hat{\omega}^2)}(1-\beta''i) - (\hat{\omega} \pm \sqrt{1-\hat{\omega}^2\beta''i})\, i \qquad \text{(A-IV-6)}$$

APPENDIX V

Boundary Layers Driven by Oscillating Basic Flow

To facilitate understanding of the thermally-driven case discussed in Section III, we consider boundary layer flow responding to an imposed, oscillating, basic state geostrophic wind with harmonic spatial variation. The following boundary conditions are applied to the system (Eqs. (III-3)):

$$u' = w' = \theta' = 0,\ v' + \hat{V}_o = 0 \quad \text{at } \eta=0$$
$$u',\ v',\ w',\ \theta' \to 0 \quad \text{as } \eta \to \text{large} \tag{A-V-1}$$

where $\hat{V}_o$ is the applied basic flow O(1). The bottom boundary conditions in Eq. (A-V-1) represent the no-slip boundary condition without temperature perturbation at the surface.

The analysis proceeds in the same manner as described in Section III. We introduce the following scale;

$$\begin{aligned} \delta &= E^{\frac{1}{2}} \\ v' &= v \\ u' &= u \\ w' &= E^{\frac{1}{2}} w \\ \theta' &= E^{-\frac{1}{2}} \theta \\ p' &= p \end{aligned} \tag{A-V-2}$$

Substitution of Eq. (A-V-2) into Eq. (III-3) yields Eq. (III-7). Therefore, the general solutions of Eqs. (III-12), (III-15) (or III-16), and (III-17) are still valid for this case when $m \ll 1$; however, the governing basic dynamics differs from that of the thermally-driven

cases. In particular, we examine only case 3 (Section III) which appears to be of most geophysical interest. That is, we consider the parameter range $m<\hat{\omega}^2(1-\hat{\omega}^2)$ and $\hat{\omega}<1$.

The lowest order scaling for the Ekman-layer, oscillatory Lineykin-layer, and thermal Stokes-layer variables for $m<\hat{\omega}^2(1-\hat{\omega}^2)$ and $\hat{\omega}<1$ is

$$
\begin{aligned}
&v_\varepsilon = O(1), \quad v_L = O\left(\left[\frac{m}{\hat{\omega}^2(1-\hat{\omega}^2)}\right]^{\frac{1}{2}}\right), \quad v_S = O\left(\frac{m}{\hat{\omega}\sqrt{\hat{\omega}}}\right) \\
&\theta_\varepsilon = O(m), \quad \theta_L = O\left(\frac{m}{\hat{\omega}}\right), \qquad\qquad \theta_S = O\left(\frac{m}{\hat{\omega}}\right) \\
&u_\varepsilon = O(1), \quad u_L = O\left(\left[\frac{m}{1-\hat{\omega}^2}\right]^{\frac{1}{2}}\right) \\
&w_\varepsilon = O(1), \quad w_L = O(1)
\end{aligned}
\qquad \text{(A-V-2)}
$$

The imposed velocity is mainly absorbed in the Ekman-layer solution and the ensuing Ekman-layer pumping drives the oscillatory Lineykin layer. The induced large temperature perturbation due to the stratification in the oscillatory Lineykin layer is absorbed in the thermal Stokes-layer solution. We notice that the vertical velocity is at most $O(E^{\frac{1}{2}})$, while the vertical velocity induced by the surface temperature forcing (see Eq. 29)) is $O(\frac{E}{\sqrt{\hat{\omega}}})$. Consequently, if $E<\hat{\omega}$ which implies that the time scale of imposed velocity field is smaller than that of turbulent diffusion, the dynamically-induced vertical motion is larger than that of thermally-driven flow. This condition is generally met in mid-latitude, diurnally-varying flows.

The complete solutions are easily obtained by applying boundary conditions in the sequence

$$v_\varepsilon = -\hat{V}_o$$

$$u_\varepsilon + u_L = 0$$
$$w_\varepsilon + w_L = 0 \qquad \text{(A-V-3)}$$
$$\theta_L + \theta_s = 0$$

The resulting solutions are quite similar to Eq. (III-29) if we replace $\frac{\hat{\Delta\theta}}{\sqrt{2\omega}}$ by $\hat{V}_o$.